Report on

Open RDA – RVP8 Signal Processing

Part 2 –Engineering Analysis with Meteorological Data

Gaussian Model Adaptive Processing (GMAP)

Clutter Filter Evaluation

Prepared by

Richard L. Ice, RS Information Systems

David A. Warde and Dale Sirmans, SI International

Darrel Rachel, Management and Engineering Technology International

WSR-88D Radar Operations Center
Engineering Branch

Norman, Oklahoma

July 2004

Executive Summary

This report describes an engineering study completed at the request of the NEXRAD Technical Advisory Committee (TAC) . This work, which analyzed the performance of a new clutter filter for the WSR-88D, was completed by the ROC Engineering Branch over a six month period with the assistance of several organizations, including the National Center for Atmospheric Research (NCAR), and the National Severe Storms Laboratory (NSSL). This study, accomplished using recorded radar time series data from several sources, is the second in a series focusing on the performance of the Gaussian Model Adaptive Processing (GMAP) clutter filter developed by SIGMET Inc. for the RVP8 radar signal processor which is to be installed in all WSR-88D radar systems beginning in 2005.

The first report in this series used simulated data to analyze performance of the GMAP filters [1]. That study verified that GMAP could meet WSR-88D performance requirements. The second study, which is the subject of this report, confirms the conclusions of the simulation study. Using radar time series data from a number of radars and for a wide range of meteorological conditions, the study team was able to verify system specification compliance.

The engineering team accomplished this work by developing a number of tools for converting data formats, for processing recorded time series data through RVP8 hardware and software systems, and for analysis. These tools and techniques are applicable to the study of other Open RDA signal processing techniques planned for the near term, and the ROC Engineering Branch will use them to validate performance of all new algorithms to be hosted on the RVP8.

The ROC engineering team continues to recommend use of the GMAP clutter filter for the Open RDA.

Table of Contents

1. Introduction 1
2. WSR-88D Requirements – Specification Summary 3
3. Engineering Analysis Methods 4
4. Project Infrastructure and Processes 5
5. Qualitative Comparisons 12
6. Quantitative Analysis 19
7. Filter Sensitivity to Expected Clutter Filter Width Input 35
8. Increase in Standard Deviation of Spectral Moment Estimate 42
9. Comparison of GMAP and the Legacy 5-pole Elliptic Filter 47
10. Summary of GMAP Performance with Real Data 53
11. Recommendations 54
12. Appendix A – References 55
13. Appendix B - Acknowledgements 56

List of Figures

Figure 1 - Clear Air Ground Clutter Suppression 13
Figure 2 - Clear Air Filtered Velocity Recovery 14
Figure 3 - Anomalously Propagated Clutter Suppression 15
Figure 4 – April 9, 2004 AP Clutter Removal - Reflectivity 16
Figure 5 - April 9, 2004 Velocity Estimate Recovery 17
Figure 6 - Clutter Suppression and AP Clutter Removal using S-pol Data 18
Figure 7 - Clutter Suppression in Severe Convective Case 19
Figure 8 - April 17, 2004 Surveillance Reflectivity Display 21
Figure 9 - April 17, 2004 Velocity Display 21
Figure 10 - April 17, 2004 Spectrum Width Display 22
Figure 11 - April 17, 2004 Reflectivity Regression, Surveillance Scan 23
Figure 12 – April 17, 2004 Reflectivity Regression, Doppler Scan 23
Figure 13 - April 17, 2004 Velocity Estimate Bias 24
Figure 14 - Feb 24, 2004 Reflectivity Display 25
Figure 15 - Feb 24, 2004 Velocity Display 26
Figure 16 - Feb 24, 2004 Spectrum Width Display 26
Figure 17 - Feb 24, 2004 Reflectivity Regression, Surveillance Scan 27
Figure 18 - Feb 24, 2004 Reflectivity Regression, Doppler Scan 28
Figure 19 - Feb 24, 2004 Clutter Region Velocity Bias 28
Figure 20 - Reflectivity/Velocity Regressions for Feb 24, 2004 29
Figure 21 - Feb 24, 2004 Velocity Bias, Non Clutter Region 30
Figure 22 -Filtered vs. Unfiltered Reflectivity, Feb 24, 2004 30
Figure 23 - April 9, 2004 Reflectivity Display 31
Figure 24 - April 9, 2004 Velocity Display 31
Figure 25 – April 9, 2004 Spectrum Width Display 32
Figure 26 - April 9, 2004 Suppression, Surveillance Scan 32
Figure 27 - April 9, 2004 Suppression, Doppler Scan 33
Figure 28 - April 9, 2004 Velocity Bias 34
Figure 29 - April 9, 2004 Velocity - Reflectivity Regression 34
Figure 30 - April 9, 2004 Velocity Bias, Convective Region 35
Figure 31 - April 9, 2004 Reflectivity Bias - Convective Region 35
Figure 32 - Suppression Sensitivity to Expected Clutter Width, April 17, 2004 37
Figure 33 - Velocity Bias Sensitivity to Expected Clutter Width, April 17, 2004 39
Figure 34 - Filter Induced Reflectivity Bias - April 17 40
Figure 35 - Filter Suppression - May 8, 2003 41
Figure 36 - Suppression Sensitivity to Expected Clutter Width, May 8, 2003 41
Figure 37 - Velocity Bias Sensitivity to Expected Clutter Width, May 8, 2003 42
Figure 38 - Reflectivity Bias Sensitivity to Expected Clutter Width, May 8, 2003 42
Figure 39 – Meteorology (KTLX Radar 152141Z), July 1, 2004 43
Figure 40 - Reflectivity B-Scan, Average of Radials 43
Figure 41 - SD Ratio, Reflectivity - Surveillance Scan July 1, 2004 44
Figure 42 - SD Ratio, Reflectivity - Doppler Scan July 1, 2004 44

Figure 43 - Velocity B-Scan, July 1, 2004 KJIM Radial 142 45
Figure 44 - Velocity SD Ratio, July 1, 2004, Doppler Scans 46
Figure 45 - Velocity Standard Deviations, Doppler Scan 47
Figure 46 - Reflectivity May 8, 2003 - Legacy Comparison 48
Figure 47 – Velocity May 8, 2003 - Comparison with Legacy Filter 49
Figure 48 - Reflectivity Scatter Grams - Filtered vs. Unfiltered 50
Figure 49 - Regression, Reflectivity to Velocity - Filtered and Unfiltered 50
Figure 50 - Reflectivity vs. Velocity Regressions, Doppler Scan 51
Figure 51 - Filtered vs. Unfiltered Velocity Regressions, Doppler Scan 51
Figure 52 - Stratiform Rain Case Filter Comparison 52

1. Introduction

- Background

This report covers methods and results of a study on the performance of the Gaussian Model Adaptive Processing (GMAP) clutter filter developed by SIGMET, Inc. and implemented in the WSR-88D Open RDA RVP8 signal processor. It reports on work performed by an engineering team in the WSR-88D Radar Operations Center (ROC) Engineering Branch. Members of the Radar Engineering Team conducted the study assisted by scientists and engineers from the ROC Applications and Operations Branches as well as by employees of the National Severe Storms Laboratory (NSSL) and the National Center for Atmospheric Research (NCAR).

- Purpose

The goal of this study is to perform an engineering study focusing on GMAP performance on actual weather radar data. The purpose is to document results of extended analysis of data produced using recorded radar data. This study is an extension of the Phase 1 Study [1] that concentrated on the use of simulations for evaluating the performance of the Open RDA RVP8 signal processor and GMAP.

- Summary of Phase 1

The Phase 1 study focused on the performance of two possible spectrum width estimators and the new GMAP clutter filters. The team used simulations based on the SIGMET A-Scope utility, taking advantage of a built in digital signal simulator. Various simulation scenarios were established to coincide with expected WSR-88D operational modes, including surveillance, Doppler, and Clear Air. The simulated data consisted of data sets (I and Q time series) generated by the simulator that were then processed through the actual RVP8 algorithms, including GMAP. The engineering team had full control of all simulation target statistics and processing parameters. The A-Scope recording capability then was used to store results in files for subsequent conversion into MATLAB.

The Phase 1 study recommended use of the R0/R1 spectrum width estimator and also concluded that GMAP met all WSR-88D performance requirements. During the course of the study, some problem areas were noted and reported to the Open RDA team and SIGMET. The engineers and scientists at SIGMET revised the GMAP and spectrum width algorithms to correct deficiencies as they were discovered and reported. The end result is a suite of algorithms that meet requirements.

- Requirement for Phase 2

The meteorological community associated with the WSR-88D accepted the results of the Phase 1 engineering study based on simulations. However, several members expressed a desire to see the work carried on with actual radar data. After receiving a detailed briefing on the results of Phase 1, the NEXRAD Technical Advisory Committee recommended use of GMAP for the Open RDA but requested a follow on study using real data. The ROC Engineering Branch accepted responsibility for conducting this study with the expectation of support from scientific elements within the various organizations associated with NEXRAD research. Subsequently, lead responsibility for the overall data quality assessment fell to the ROC Application Branch with members of Operations and Engineering supporting. A joint team consisting of members of those groups as well as the Radar Engineering team was formed to address the study. The study plan [6] called for an engineering study as a subset of the overall effort. This report documents results of the engineering portion of the study.

- Project Time Line

The GMAP evaluations have been conducted during Open RDA development and testing efforts. The initial simulation phase occurred from September 2003 through January of 2004. One major goal of that study was to identify if there were any technical issues that might prevent the use of GMAP for the ORDA. None were found and the NEXRAD Technical Advisory Committee recommended that GMAP be further developed for use in the ORDA.

The second phase began in February 2004. This second study focused on the use of real radar data and continued through July of 2004. The end of the second phase was to be coincident with the start of formal ORDA system testing.

2. WSR-88D Requirements – Specification Summary

WSR-88D Clutter Filter performance requirements were summarized in the Part 1 study [1] and are repeated here.

Ground clutter suppression requirements are established in section 3.7.1.7.1 of the NTR (SS section 3.7.2.7.1). General requirements applicable to any suppression method are:

- A clutter suppression capability of at least 30 dB in the reflectivity channel.

- Clutter suppression selectable between 20 dB and 50 dB in the Doppler channel.

- In areas where the clutter suppression is <u>not</u> applied, there shall be no degradation in the weather return parameter measurement accuracy with respect to the NTR or SS requirements (SD[V] $\leq$ 1 ms^{-1}, SD[W] $\leq$ 1 ms^{-1} and SD[Z] $\leq$ 1 dB).

  Meteorological signal estimate errors due to the clutter suppression are addressed in section 3.7.1.7.2 of the NTR (SS section 3.7.2.7.2). General requirements are:

- Bias and standard deviation contributions by the clutter suppression device to the mean radial velocity and spectrum width estimates shall be less than 2 ms^{-1}.

- The test conditions given in the NTR and SS are specific for a notch filter. General case test conditions are SNR > 20 dB, SCR > 30 dB i.e. high signal with low clutter conditions.

The NTR and SS specifications for reflectivity bias are specific for a notch and not applicable to the GMAP method since GMAP reconstructs the spectra and removes the bias associated with clutter suppression. What is applicable in this case is the specification for the post filter reflectivity bias correction algorithm, which has a goal of correction uncertainty of less than 2 dB.

3. Engineering Analysis Methods

Prior to this study, GMAP performance assessment was based on simulated data. Use of simulations is advantageous because the input weather and clutter spectrum data can be controlled fully by investigators. Statistical parameters of the input test signals can be set for any values of mean and standard deviation appropriate for the analysis. This was sufficient for bounding the expected performance of the signal processing algorithms, and for judging quantitatively how well the various processes meet system specifications. Simulated data is less useful for judging overall quality of the meteorological estimates that would be produced by an operational system. This is best done with actual weather input data generated by the hardware associated with the system, either from real time operations, or reconstructed from archived data.

The archived data typically consists of two types, or levels. Level 1, or time series data, is the digitized output of the radar receiver, and is comprised of digital versions of the in-phase (I) and quadrature-phase (Q) components of the detected return signals. Level 2, or base moments, are the basic output of the signal processor and are created from Level 1 data with suitable algorithms and relevant processor set-ups. The Level 2, or base data product, is also more applicable when teams of meteorologists are called upon to judge the utility of the output data.

This project employed both Level 1 and Level 2 data for the analysis. The next section of this report documents the sources of these data sets and discusses relevant issues. Typically, Level 1 (time series) data sets were used to produce level 2 outputs using a playback mechanism in the RVP8. At times, the Level 2 outputs were obtained directly from the radar systems. Comparison Level 2 data sets from the National

Weather Service National Climactic Data Center (NCDC) were also used where applicable.

Data products were used in this study to verify the simulator performance and to evaluate the GMAP filter's effect on clutter and weather signals in a quantitative manner. The primary tool for detailed analysis was MATLAB [3]. The Level 2 base moments generated by the RVP8 playback process, along with some Level 2 data from the NSSL KOUN radar, were converted into MATLAB data format for processing. The primary analysis tools within MATLAB were regressions and histograms. MATLAB was also used as a visualization tool and most base products depicted in this report were generated in the MATLAB environment.

4. Project Infrastructure and Processes

- ROC Engineering New Science Plan

This work was conducted in accordance with an internal project plan delivered to ROC Engineering in August 2003 [5]. This plan described the goals for evaluating all near term enhancements planned for the Open RDA era, including Range-Velocity Ambiguity Mitigation, increased data resolution, and over sampling. The plan discussed in some detail the sources and types of data needed and the associated tools. Most of the items identified in the plan were implemented in the course of the GMAP evaluation.

- Supporting Participants

This work was accomplished with the help of many organizations and individuals in the WSR-88D community. As with any large technical project, no one person or group possesses the knowledge or resources to complete the job alone. A key to success for this phase of the GMAP project was the acquisition of adequate radar data sets. NSSL, NCAR and the OST Open RDA RSIS contract team were especially helpful in providing suitable data sets. Support contract members of the ROC Engineering Branch also contributed data and data processing support. Appendix B lists all supporting organizations and individuals who assisted with this effort.

- Laboratory Network

The engineering team set up a laboratory network at the ROC South location consisting of several Linux workstations, the ORDA RVP8 and RCP8 processors, and a mass storage system based on a Redundant Array of Independent Disks (RAID).

- Software Tools

The team used a mix of commercial software packages and developed tools. The primary analysis tools were developed in MATLAB. Some previously available FORTRAN code utilities were also used, most notably a routine for converting WSR-88D level 2 data into MATLAB.

- Data Sources

Time Series – Key to the real data analysis was the availability of time series data from a number of sources. Replaying time series data is the most flexible means for analyzing signal processor performance because engineers can adjust processing parameters to focus on particular features and can control parameters such as clutter filter settings. Some parameters are of course not changeable since they are set at the time of data collection. Examples of these are PRF, wavelength, and pulse width. Engineers also must have a good understanding of the values of system noise levels and overall gain constants that existed in the radar at the time of collection although some adjustments to these values can be made without compromising the value of the processed data. This project made use of time series data from four very different sources.

L1RP – A major source of time series data was from the ROC Engineering developed Level 1 Record and Playback (L1RP) suite. This utility consists of a client/server software system designed to run in the RVP8 environment. A small, efficient server task runs on the RVP8 to access the time series data using the SIGMET API. A client is installed on another machine typically for capturing the data via the network connection, although small amounts of data can be stored locally on the RVP8 disk. Data was transferred via a laptop computer, jump drives, or a large capacity portable disk drive. ROC engineers also developed a

modified RVP8 major mode for playing back the time series data off line on a separate RVP8/RCP8 combination. The team used this process for capturing data from the KJIM ORDA test bed and also used this method for capturing data from the NCAR S-pol radar.

NSSL RRDA – Team members analyzed a significant number of cases collected by NSSL using the KOUN Research RDA (RRDA). NSSL engineers collected these sets over nearly a two year period using the legacy analog receiver and the RRDA signal processor. Most of the data collection occurred during the JPOLE exercise but some specialized data sets to support the RV mitigation and super resolution projects were collected. In addition, NSSL collected some data especially for the GMAP evaluation effort, most notably a stratiform rain case on February 24, 2004. The RRDA data format is different from the L1RP format.

TS Archive – While this project was in progress, SIGMET released an improved version of their time series recording and playback utility, namely, TS Archive. This is a very powerful and flexible suite of software that captures any amount of time series data within the RVP8 along with all relevant signal processing parameters. It also features a convenient file management and playback capability. One drawback to TS Archive is that it was not initially compatible with SIGMET's IRIS software, precluding convenient display of processed radar data. ROC Engineering made the decision to use SIGMET's TS Archive for all future time series collection and play back, although it was not used extensively for this study.

Legacy A1DA – In the mid 1990's ROC contracted with NCAR to develop a legacy time series recording and playback system, the Archive 1 Data Analyzer (A1DA). While the A1DA is no longer in use, a few data sets are still available, the most well known being the May 3, 1999 OKC tornado. For this study, a case containing anomalous propagation collected at Memphis TN was used.

Level 2 – Level 2 data is the output of the signal processor composed of reflectivity, velocity, and spectrum width base moments. Level 2 was either generated during the RVP8 play back process, obtained from NSSL, or from NCDC.

NSSL RRDA – The ROC engineering team had no capability to process time series data into level 2 data using the legacy clutter filters. NSSL has such a tool which is essentially an off line emulation of the entire legacy processing suite. The ROC team requested at least two level 2 data sets from NSSL processed using the legacy 5 pole elliptic filter. Also, NSSL provided a level 2 file for each level 1 data set for use with the RRAT display and analysis program, these files are used for viewing the base data in RRAT to identify features of interest. NSSL provided several utilities for using RRDA level 2 data and assisted with system configurations and data translations.

WSR-88D Level 2 – The team used WSR-88D level 2 formatted data as the primary means for ingesting base moments into MATLAB. This was accomplished using a utility previously developed by ROC Software Engineering. For data generated during RVP8 playback, WSR-88D level 2 data was obtained through the use of an IRIS output pipe developed by SIGMET for the ROC in 2003. An initial problem with this data occurred when team engineers failed to notice that the RVP8 was not set up to range average four 250m reflectivity cells into a single 1 km reflectivity cell. This was because the output of the IRIS pipe was producing data at 1 km increments. The result was that early displays of reflectivity data were extremely grainy in appearance. The IRIS pipe merely selects every fourth reflectivity estimate for the output. Once range averaging was invoked within the RVP8, the data appeared much smoother, however the IRIS pipe still only selected every fourth reflectivity estimate for the output. Team engineers were able to convert NSSL RRDA level 2 data into WSR-88D level 2 data as well as obtain WSR-88D level 2 data from the NCDC for comparisons. These comparisons were done using data from KTLX in Oklahoma City as well as the KNQA radar from Memphis. Primary purposes of these

comparisons were to check calibration values and for double checking data time stamps.

SIGMET RAW Files – The engineering team also used data coming directly from the RVP8 in SIGMET native format. This was done to bypass use of the IRIS output pipe due to limitations in the pipe, specifically the issue of producing reflectivity data at 1 km increments only. A team member created a special conversion routine to ingest SIGMET format level 2 data into the MATLAB working environment.

- Meteorological Data Cases Reviewed

The team began by researching all available meteorological cases for which compatible time series data was available. Over the past couple of years, NSSL has systematically collected both moment estimate data as well as limited amounts of time series data. Most of this data was obtained in support of the dual polarization project and for the development of mitigation techniques to address the problem of range velocity ambiguities. NSSL also obtained some special data collections in support of the super resolution studies. The team reviewed available data cases and requested the following samples from NSSL for the initial investigations:

- 10/08/2002 – Stratiform Rain with Bright Band
- 10/28/2002 – Asymmetric Squall Line
- 02/13/2003 – Stratiform Rain
- 04/05/2003 – Scattered Storms
- 05/08/2003 – Tornados
- 06/11/2003 – Squall Line over Radar
- 02/23/2004 – Widespread Stratiform Rain

These data sets served to familiarize the team with general behavior of GMAP and for developing detailed conversion and analysis tools. The two most useful data sets were the May 8, 2003 tornado and the February 23 – 24, 2004 widespread stratiform rain cases. These two sets in particular were used in the quantitative analysis portions of the study, and were especially appropriate for comparing performance of the legacy filter to

GMAP. In addition to the above data sets, NSSL collected a special clear air case for the ROC team on March 16, 2004.

The team also used the KJIM radar for some special data collections. Once the Open RDA system was installed and operating, engineers used it to control the ROC's test bed antenna and collected data on several occasions. These special data collections comprise the bulk of the cases used for detailed quantitative analysis. Of particular importance were data sets collected on April 9, April 17, and July 1, 2004.

Data Translations

RRDA time series to L1RP – Two ROC engineers had previously created a utility for converting the NSSL KOUN radar time series data into the ROC's L1RP format for playback. This utility proved quite useful as the majority of the time series data available initially was from KOUN.

Legacy A1 to L1RP – A member of the ROC's Software Engineering Team developed a special utility for converting data recorded with the legacy Archive 1 Data Analyzer (A1DA). The team used this utility to convert and playback data sets from the May 3, 1999 OKC tornado and a special data set containing AP clutter obtained in the summer of 1997.

WSR-88D Level 2 to MATLAB – A ROC Software Engineering Team member had previously created a utility for ingesting standard WSR-88D level 2 data into MATLAB. For this project, he updated the tool and assisted team members with installation and running the program. This capability proved very useful for obtaining WSR-88D products for comparison as well as for handling legacy processed data from NSSL.

RRDA Level 2 to MATLAB – This conversion turned out to be a little more complex. NSSL provided a tool for reading RRDA Level 2 data into the Linux based Open RPG. Once within the ORPG environment, team members were able to make a standard WSR-88D level 2 recording which could then be ingested into MATLAB using the tool described in the paragraph above.

SIGMET Level 2 to MATLAB – Because of problems in using the SIGMET developed IRIS WSR-88D Level 2 Output Pipe, a team member developed a new routine for converting the internal RVP8 level 2 outputs into MATLAB. This freed engineers from restrictions associated with the IRIS pipe and paved the way for future analysis of such techniques as super resolution.

RVP8 Playback

The process of time series playback is complex in the RVP8 environment and a few notes on the methods are appropriate here. The initial capability for ingesting time series data and producing output moments was developed by two ROC team members who modified RVP8 code, creating a special user major mode. This was the tool used for all playback producing the data in this report. During the time period of this study, SIGMET modified the RVP8 code, updating it to support a new time series recording and playback capability known as TS Archive. Unfortunately, the updated software was not compatible with the ROC developed playback methods forcing the evaluation team to keep their RVP8 held at an older version of the code. This restriction did not affect results of the study.

SIGMET and the ROC worked together to resolve the recording and playback issues. The expectation is that a fully functional TS Archive record and playback system, compatible with the ORDA software suite, will be available for future studies.

NSSL Research Radar Analysis Tool (RRAT)

NSSL provided their RRAT software [7] to assist the ROC in sorting and analyzing the time series data obtained from KOUN. RRAT was installed with NSSL assistance on the same Linux workstation that hosted the Open RPG. This software is capable of displaying both the meteorological moments (reflectivity, velocity, and spectrum width) and the spectrum of the associated time series samples for each selected range gate. RRAT proved extremely valuable in identifying suitable data cases and features within those data cases which were relevant to the GMAP analysis.

Linux Open RPG

Members of the ROC Software Engineering Team installed a Linux Open RPG on one of the workstations set up for this project. The ORPG was used to sort and analyze level 2 data produced by the RVP8 playback process, for displaying level 2 data obtained from NCDC, and for converting NSSL RRDA level 2 data to WSR-88D level 2 data formats.

5. Qualitative Comparisons

Early study efforts focused on qualitative assessments in order to identify promising cases, validate data collection and playback processes, and to develop necessary tools. As part of this process, the engineering team generated a significant number of images comparing radar moments processed with and without the GMAP filters applied. This section contains a sampling of the images obtained. These are used for qualitative assessment and for gaining insight into the behavior of GMAP. A subsequent section of this report documents the more thorough quantitative evaluations conducted on selected data cases.

- Clear Air Clutter Suppression and Velocity Recovery (March 16, 2004)

On March 16, 2004, the NSSL team collected some time series data for the ROC team. The goal was to obtain a good clear air case, under conditions appropriate for generating a clutter map. A case of this type is potentially useful for evaluating various clutter map generation schemes and for collecting statistical data on expected clutter spectrum widths. Conditions on March 16 were generally good for this purpose except for the winds being slightly higher than desired.

NSSL recorded time series data using the KOUN research radar, the legacy analog receiver, and the RRDA time series recorder. The ROC team converted the RRDA time series to L1RP format and processed the data set through the RVP8. The RVP IRIS output conversion pipe was then used to produce WSR-88D Level 2 data, which was then ingested into the Linux Open RPG for viewing using the base data

display. Figure 1 depicts a comparison of the reflectivity for filtered and unfiltered processing.

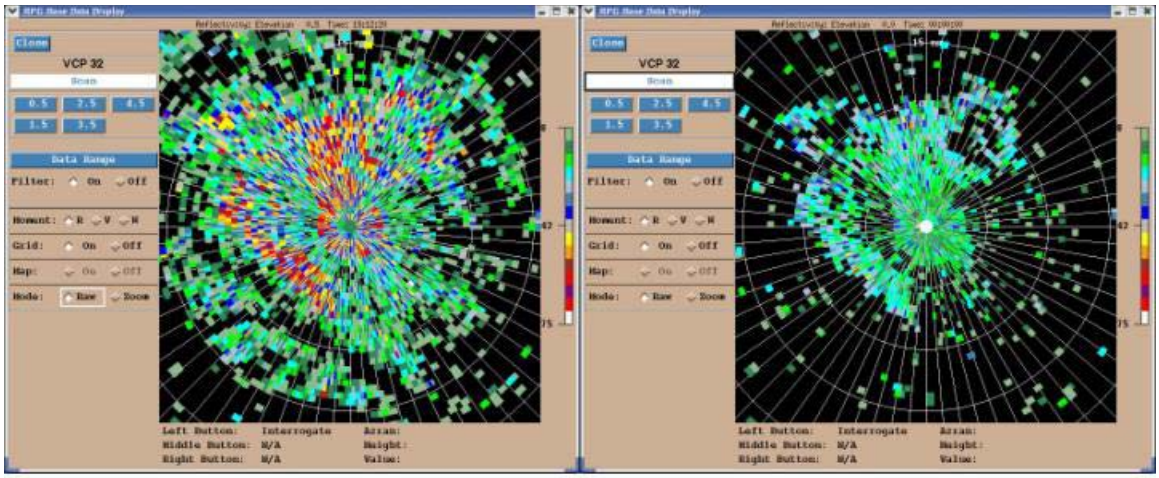

(a) Unfiltered Reflectivity (0 to 20 NM) (b) GMAP Filtered Reflectivity

Figure 1 - Clear Air Ground Clutter Suppression

As can be seen, a significant amount of ground clutter is removed by the GMAP filters, with clutter residue levels in (b) primarily below about 25 dBz. This data shows GMAP easily meets the reflectivity channel suppression requirement of 30 dB. Processing this data set and viewing results enabled the engineering team to gain experience with data handling and to ensure proper configuration of the RVP8 signal processor and operation of the playback software.

An example of velocity moments processed with and without GMAP is shown in the next figure.

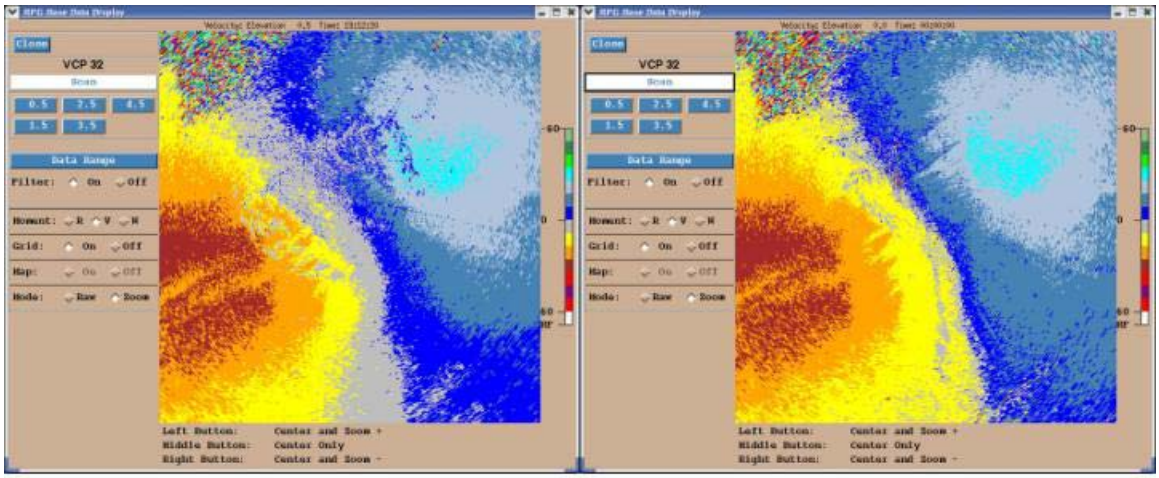

(a) Unfiltered Velocity (0 to 20 NM) (b) GMAP Filtered Velocity

Figure 2 - Clear Air Filtered Velocity Recovery

The left panel (a) shows the velocity base product for the unfiltered case. Contamination from ground clutter can be seen in the center portions of the display. The panel on the right shows the results when the GMAP filter is applied everywhere. Most of the contamination from the ground clutter is eliminated and the zero isodop line is more pronounced. The area indicated as near zero is much narrower. This indicates that GMAP does produce a velocity bias along the zero isodop as observed in the simulation studies. However the velocity display is much cleaner and the wind field is more easily observed in the filtered case.

- Examples of Anomalously Propagated Clutter Suppression

The GMAP filter will also need to be applied by network operators in locations where AP clutter occurs. This is typically a situation where the clutter appears in areas not served by a clutter map so the filters are not automatically applied as in normally propagated ground clutter. In cases where GMAP is applied to a region of AP, it is expected that the filter will work as well as for normal clutter. Unfortunately, there are very few cases of AP clutter where time series are available. One such case occurred in Memphis TN on June 28, 1997. An NCAR engineering team captured Level 1 time series data for this event using the legacy Archive 1 (A1) recorder developed under a ROC research task. NCAR made this data available.

The ROC engineering team was able to convert the older A1 format time series into the L1RP format for playback on the RVP8. The following figure depicts the results as seen on the SIGMET IRIS real time display for both non-filtered and GMAP filtered reflectivity.

Figure 3(a) display shows reflectivity processed from the KNQA time series without any filtering. The NCAR team was only able to capture a portion of a scan for each case due to hardware limits of the A1 recorder, thus only a portion of the elevation cut is processed. In this unfiltered case, a significant amount of AP clutter is seen immediately to the east and south east of the radar with smaller amounts of extended AP occurring over most of the eastern half of the display. Figure 3(b) shows the results when GMAP is applied everywhere. It can be seen that clutter from the AP condition is significantly reduced while the real weather return is essentially unaffected.

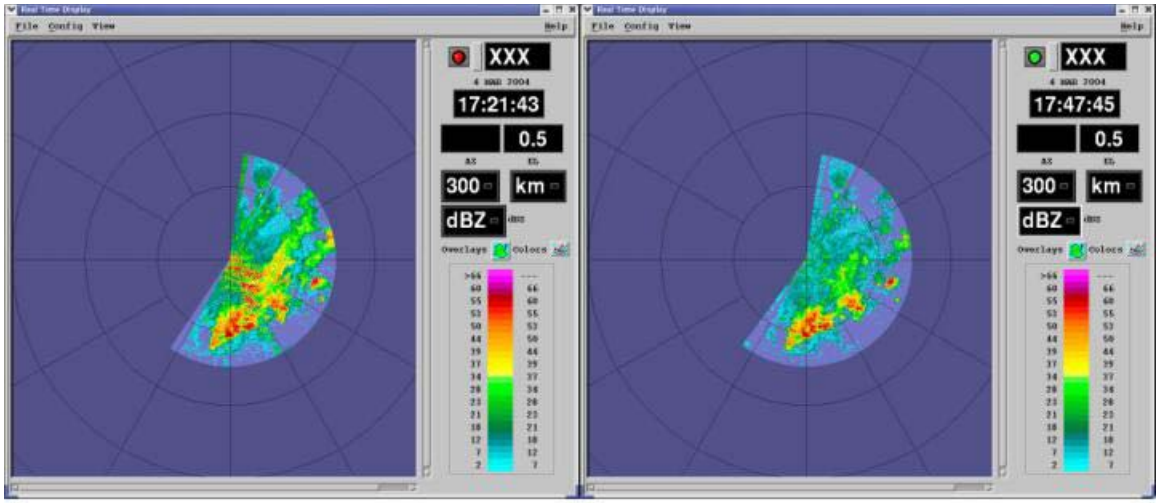

(a) Non Filtered Reflectivity (b) GMAP Filtered Reflectivity

Figure 3 - Anomalously Propagated Clutter Suppression

On April 9, 2004, the ROC team collected L1RP time series data from the ROC's KJIM radar. This system had been fitted with an operational Open RDA RVP8 processor. The weather on April 9th was quite active with fairly widespread thunderstorms and rapidly changing atmospheric conditions. The team collected data aimed at evaluating GMAP performance in convective conditions, but upon processing the data, discovered that some AP clutter conditions had also occurred. This data set is

examined in more detail in following sections, but here we focus on the GMAP filter performance in suppressing normally propagated as well as AP clutter. Figure 4 shows a close up view of the non-filtered reflectivity field along with the result from applying the GMAP filter.

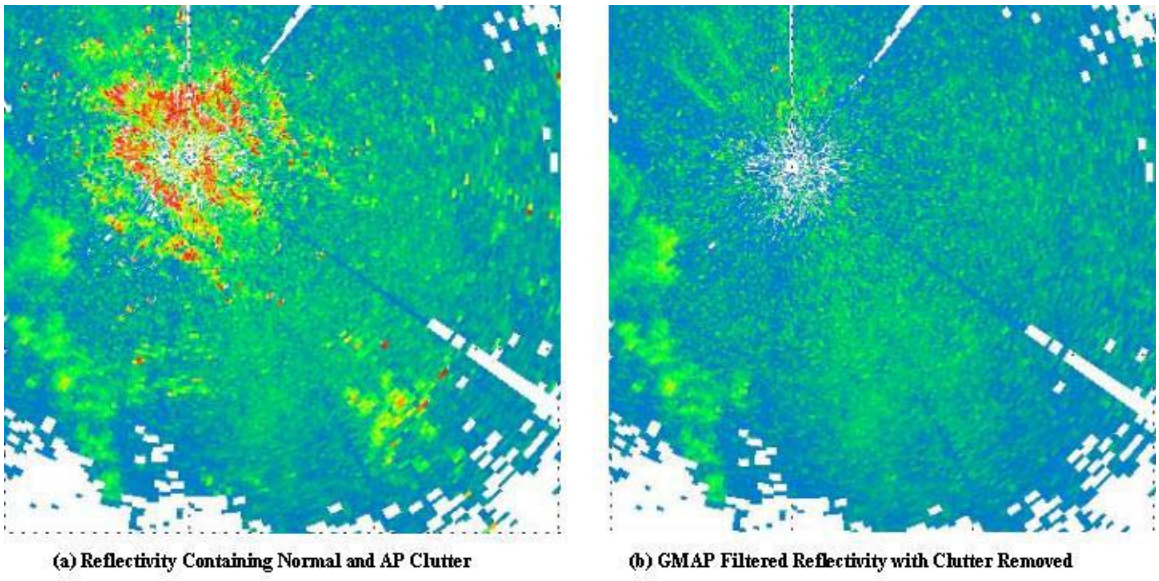

Figure 4 – April 9, 2004 AP Clutter Removal - Reflectivity

In the above figure, the large reflectivity values due to close in ground clutter are observed near the radar (upper left quadrant in Figure 4(a)). A moderate patch of AP clutter is seen to the south east as well as a few randomly occurring spots of AP clutter in a number of other locations. Figure 4(b) shows the same data, processed through the GMAP clutter filter. As seen, the AP patch is essentially eliminated and there is very little remaining clutter residue from the near-in ground clutter.

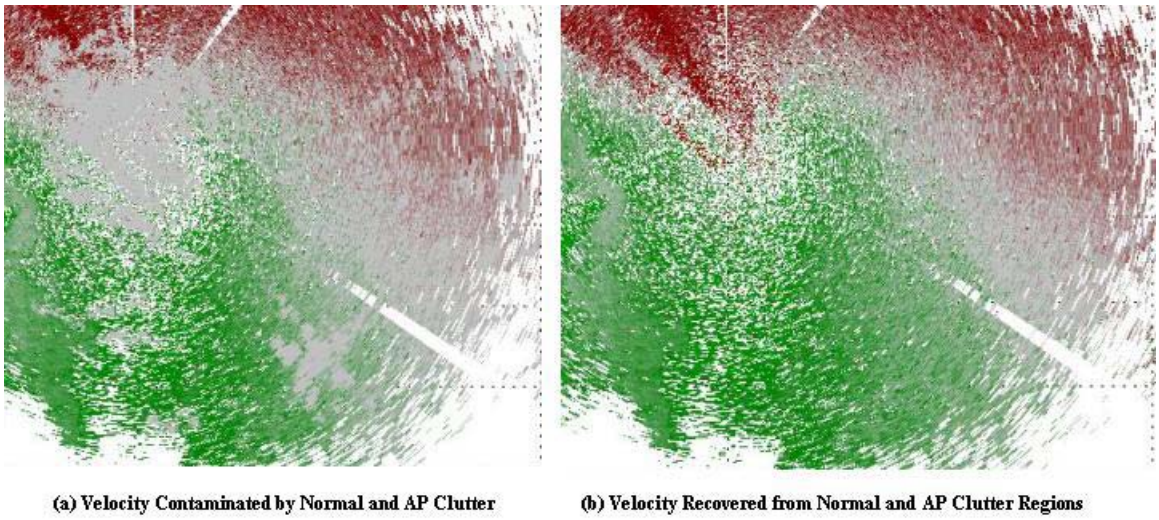

Figure 5 - April 9, 2004 Velocity Estimate Recovery

Figure 5 shows the equivalent velocity estimates for filtered and unfiltered conditions. Figure 5 (a) is a close up image of the velocity field contaminated by ground clutter. Note the zero mean velocity estimates associated with the patch of AP clutter. In the panel to the right, the velocity estimates are cleaned up by the GMAP filtering process, with usable estimates displayed in regions previously contaminated by both the normally propagated and AP clutter regions.

The next figure represents a case study using data from the NCAR S-Pol radar located near Boulder CO. S-Pol is a transportable dual polarization radar operating at S Band and has similar characteristics to the WSR-88D [4].

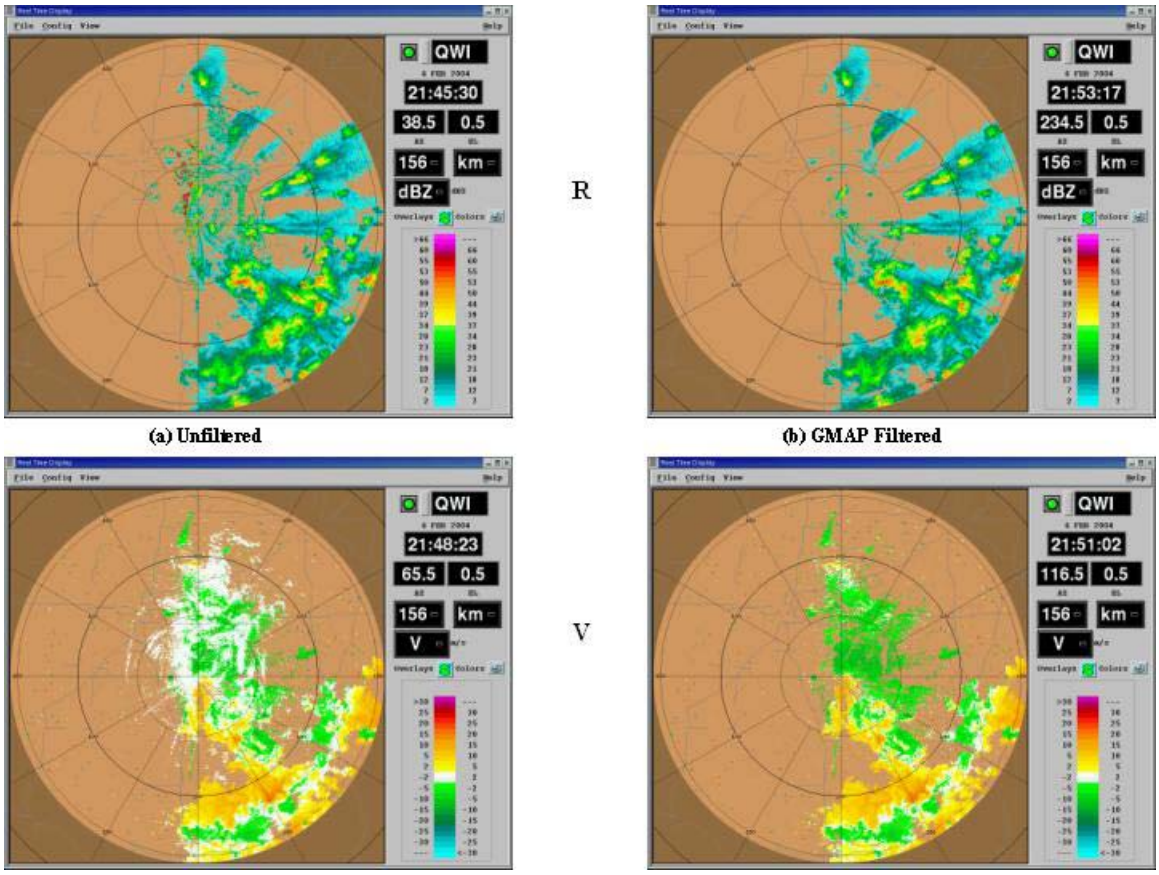

Figure 6 - Clutter Suppression and AP Clutter Removal using S-pol Data

The images in Figure 6 were generated in one of the ROC's RVP8's using time series data obtained from NCAR. The engineers at NCAR used the ROC's L1RP time series recording software. S-Pol collects data in a slightly different manner than a conventional WSR-88D, for example receiver samples are collected at 150 meters rather than at 250 meters as in the WSR-88D. Nonetheless, this data is useful for observing the GMAP clutter filter effects. This is a good data set because of the location near the Front Range, which provided a severe clutter environment, and the particular weather situation yields some insight into filter performance.

In Figure 6(a), the reflectivity and velocity products are shown for the non-filtered case. Note the high reflectivity returns to the immediate west and north west of the radar. These are ground clutter returns from the mountains. There is also considerable clutter for quite a distance to the north. This is analyzed as clutter because of the corresponding low mean velocities depicted in the velocity display (white areas). On the right side of

the figure (b), the two panels depict results from applying the GMAP filter everywhere in the field. Note that the areas previously identified as clutter are eliminated, non-clutter weather signals are unaffected, and there is extensive velocity estimate recovery.

- GMAP Performance in Severe Weather

Data from the May 8, 2003 Oklahoma City and Moore Oklahoma tornado was used to examine GMAP performance in a severe weather case. This was a particularly good case since a severe tornadic storm passed within just a few miles of the radar, with significant portions of the storm occurring in a ground clutter environment. Figure 7 shows a reflectivity analysis for one scan of the storm.

In (a) of Figure 7 the unfiltered reflectivity is plotted in a MATLAB display, the fact that nearby ground clutter obscures a portion of the storm is quite obvious. In fact, even though the storm was producing at least an F4 tornado at this time, it is hard to detect the hook echo associated with it. Panel (b) shows the same data, but filtered with GMAP. Most ground clutter is removed and the hook echo can now be seen clearly.

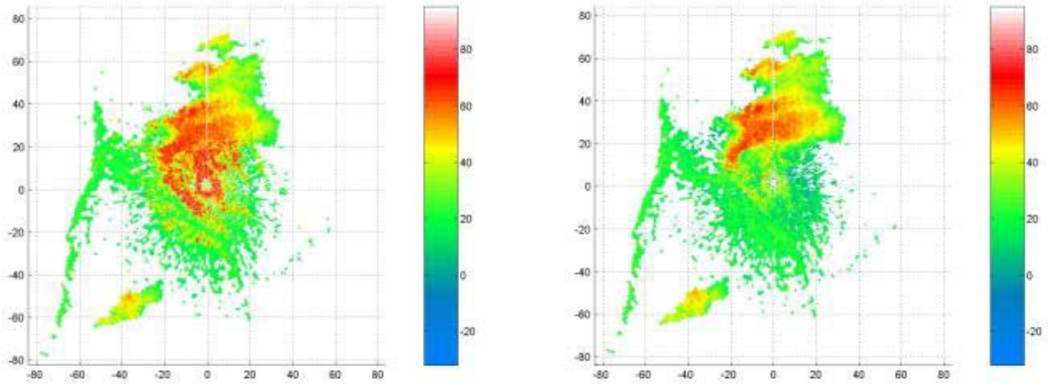

Figure 7 - Clutter Suppression in Severe Convective Case

6. Quantitative Analysis

This section is focused on analyzing measurable performance of the GMAP process with respect to requirements. While the previous qualitative survey lends insight

into the algorithm performance and its impact on data quality, only such a quantitative approach can yield an assessment of the GMAP filter's ability to meet performance requirements.

- Regression Analysis Notes

Statistical methods are used in most the data analysis. Regressions are used extensively since this is a convenient way to identify relationships between two statistical populations such as filtered and unfiltered data fields. Population histograms and associated moments are used in calculations of some signal characteristics such as expected value and estimate standard deviation.

Most of the analysis used an initial or "seed" clutter width of 0.3 ms^{-1} although it is shown in section 6 and in the simulation study [1] that the seed width has little effect on suppression performance.

- Clutter Suppression Determination

Comparing reflectivity fields using clear air data can produce a simple analysis of clutter suppression. Figures 8, 9 and 10 depict close in clear air images for data that has been both unfiltered and filtered with GMAP. Note the difference in reflectivity returns (Figure 8). The difference between these fields should be a fair measure of the amount of clutter suppression.

- Case 1 – Clutter with Weak Clear Air Return (April 17, 2004)

The filtered and unfiltered data from the case of April 17, 2004 is shown in Figures 8 through 13. Figure 8 is a comparison of the unfiltered and filtered reflectivity Note the clutter reduction in the reflectivity field magnitude due to clutter removal while the clear air return meteorological signal is unaffected. A small amount of clutter residue is visible in Figure 8(b).

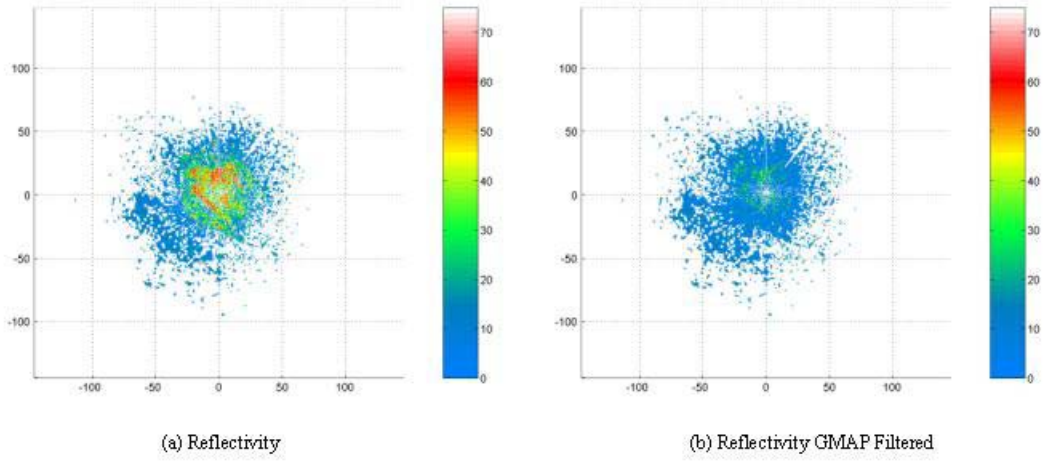

Figure 8 - April 17, 2004 Surveillance Reflectivity Display

Figure 9 is a comparison of the velocity estimate for both the filtered and unfiltered case. In Figure 9(a), significant portions of the velocity estimates are zero, indicating clutter contamination of the estimates. Figure 9(b), the GMAP filtered output indicates a significant increase in valid velocity estimates.

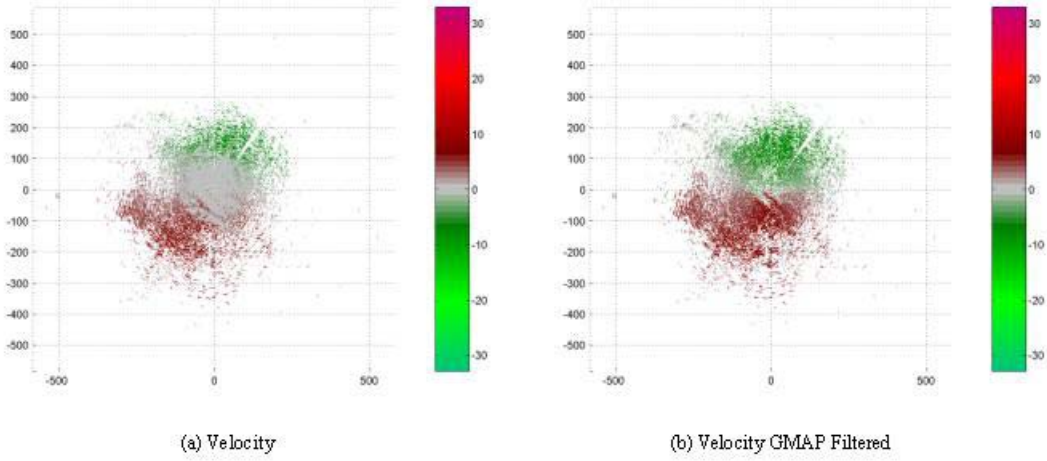

Figure 9 - April 17, 2004 Velocity Display

Figure 10 depicts the spectrum width fields for both unfiltered and filtered results. Similar to the velocity images, the unfiltered width product exhibits significant portions of the data at extremely low values, as expected from ground clutter contaminated

returns. In fact, the general shape of the Norman OK ground clutter is defined by the many dark gray, or zero value, returns as seen in Figure 10(a). Figure 10(b), the filtered output, shows a significant reduction in the estimate output of zero width, although the values are still quite low, as expected with the clear air return field.

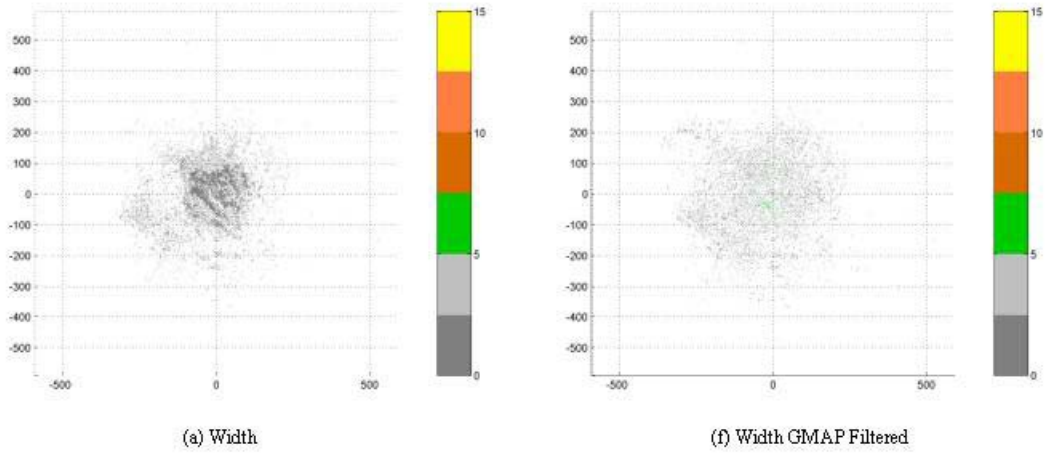

Figure 10 - April 17, 2004 Spectrum Width Display

The level 2 data from this set formed the input for a series of quantitative evaluations, using MATLAB tools to plot various aspects of the data statistics.

Regression of the filtered data on the unfiltered data is shown in Figure 11 for the surveillance scan and Figure 12 for the Doppler scan. The unfiltered data is the clutter plus signal and the filtered data is the clutter residue plus signal. The red dashed line represents a difference between the filtered and unfiltered scales of 50 dB. From the scatter gram position relative to the 50 dB line and the residue field in both Figures, it is seen that clutter is suppressed to well below the signal level for clutter to signal levels over 50 dB.

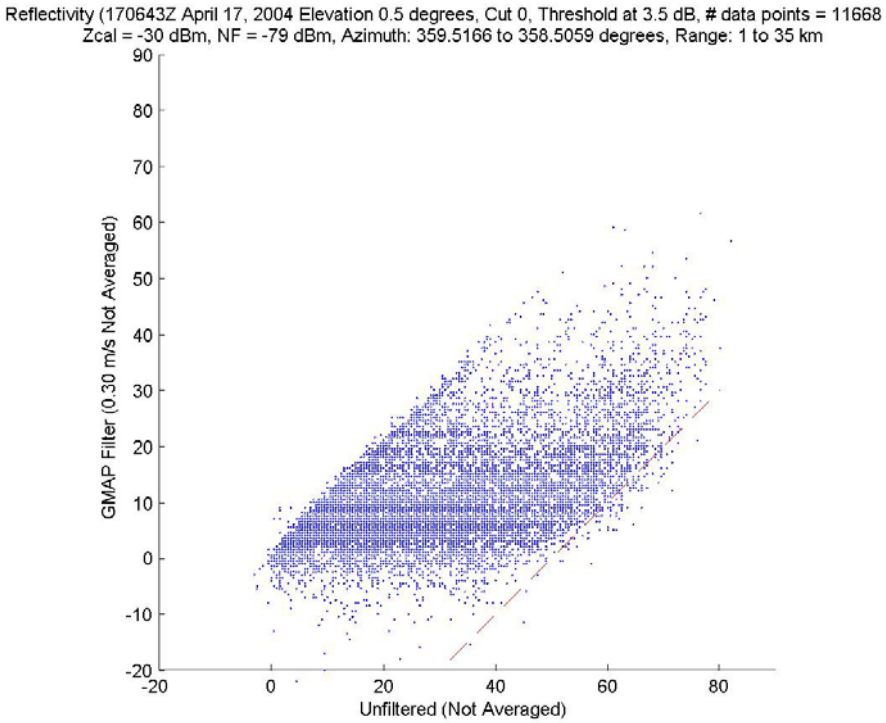

Figure 11 - April 17, 2004 Reflectivity Regression, Surveillance Scan

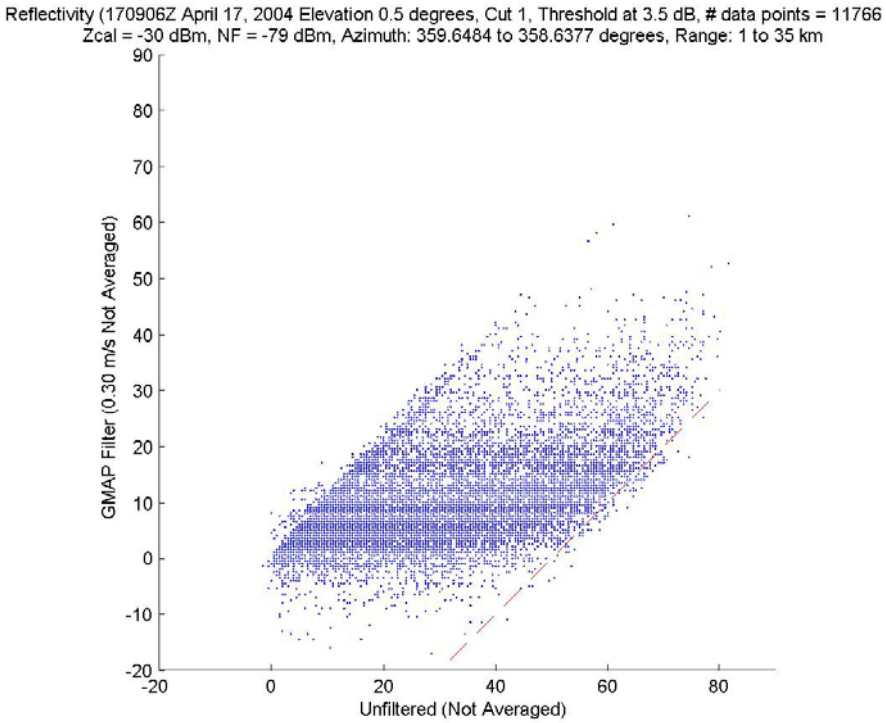

Figure 12 – April 17, 2004 Reflectivity Regression, Doppler Scan

Signal velocity bias induced by the clutter filtering is shown in Figure 13. The solid line is the vertical axis mean value (filtered velocity). The stratified output region along the zero velocity input region are signals recovered by the filtering or clutter signals reduced to below noise level. Maximum velocity bias is about 2.7 ms^{-1} and occurs at an input velocity of about 1.0 ms^{-1}. Although peak bias is larger than the specification of 2.0 ms^{-1}, this case of strong clutter and weak signal was identified as an exception in the Part 1 simulation study [1]. In fact, using clutter model A of the System Specification (NTR), the minimum usable velocity is 4 ms^{-1} when providing 50 dB of suppression with an expected spectrum width of the meteorology of 4 ms^{-1}. As can be seen, the GMAP filter provides less bias for velocities greater than 4 ms^{-1}. The bias does not exceed 2 ms^{-1} until the velocity falls to nearly 1 ms^{-1}. Thus GMAP meets system requirements for velocities up to 3 ms^{-1} less than the minimum usable velocity specified in the NTR for this case.

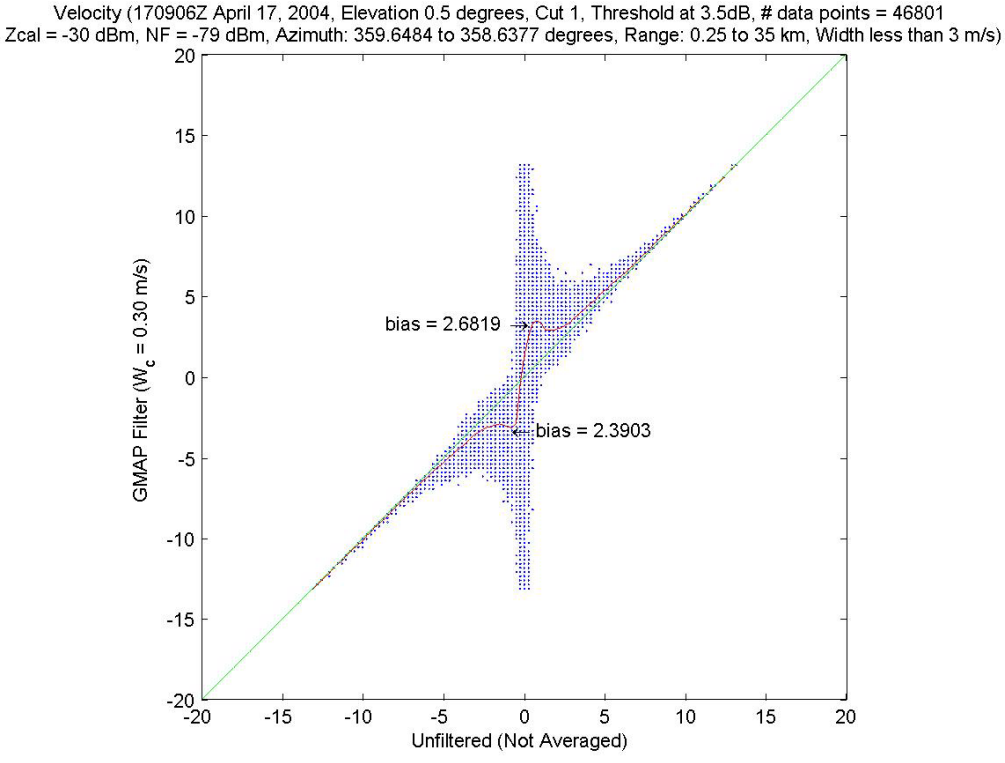

Figure 13 - April 17, 2004 Velocity Estimate Bias

- Case 2 – Clutter with Moderate Meteorological Signal (February 24, 2004)

A case with moderate clutter to signal ratio is shown in Figures 14, 15 and 16. This data was from the NSSL KOUN Research Radar (RRDA), with the level 2 moment estimates being generated from time series collected by NSSL personnel using the RRDA proof of concept Archive 1 device. The data originated through the legacy analog IF receiver and A/D converter. Thus this set of time series data is not necessarily representative of data that would have been obtained from the Open RDA's RVP8 digital receiver, but is still useful for analyzing clutter filter performance.

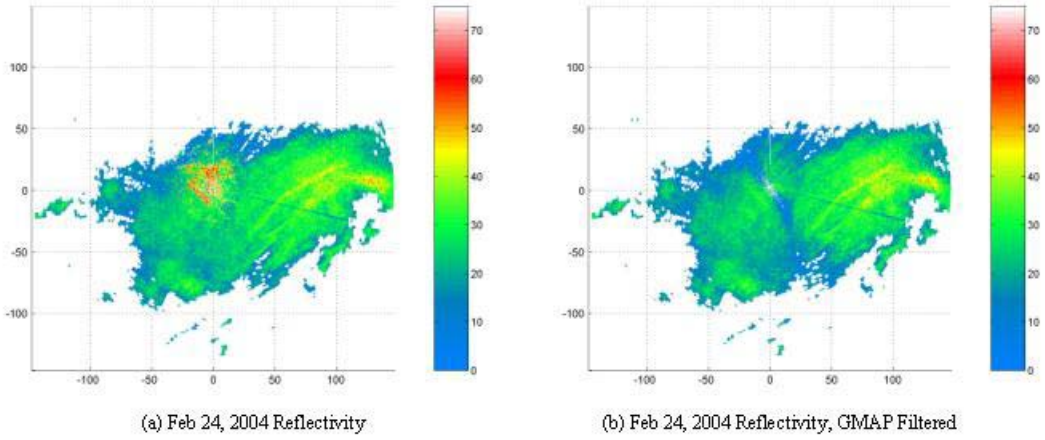

Figure 14 - Feb 24, 2004 Reflectivity Display

Note from the reflectivity displays (Figure 14) that there is little visible clutter residue. The data exhibits a negative bias along the zero isodop as expected from previous simulations due to the extremely low spectrum widths in this case.

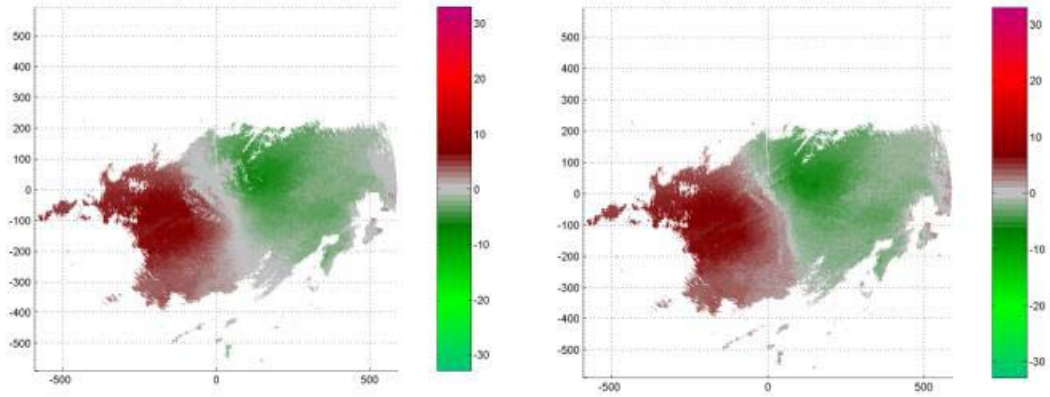

(a) Feb 24, 2004 Velocity (b) Feb 24, 2004 Velocity, GMAP Filtered

Figure 15 - Feb 24, 2004 Velocity Display

From the velocity displays (Figure 15), note the area recovered in the clutter region. Also note the reduction in the zero isodop (the region between dark red and green) in the filtered velocity display. This is due to the velocity bias induced by the filter. Normally the filter will not be operating outside the clutter region but it may be switched on if anomalously propagated clutter signals are present. Spectrum Width is shown in Figure 16.

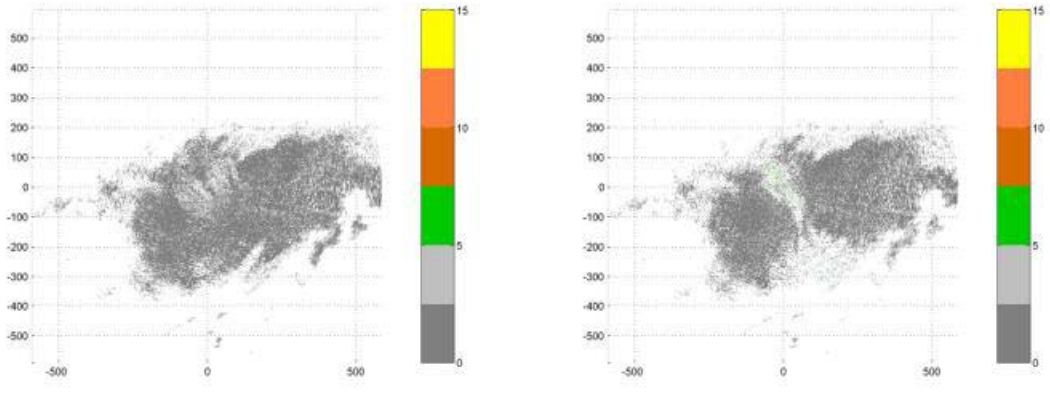

(a) Feb 24, 2004 Spectrum Width (b) Feb 24, 2004 Spectrum Width, GMAP Filtered

Figure 16 - Feb 24, 2004 Spectrum Width Display

Note from the reflectivity and spectrum width displays that GMAP does not perform well along the zero isodop in the clutter region due to the large clutter to signal ratio and the resulting clutter residue. Reflectivity and velocity estimates are sensitive to clutter residue greater than about 10 dB below the signal whereas spectrum width is

sensitive to residue greater than about 20 dB below the signal. This type of behavior is also observed in the legacy filters.

The regression scatter plots for the 0.5-degree surveillance and Doppler scans are shown in Figure 17 and 18. The observed suppression appears to be less than the previous and following cases. Possible causes include large phase noise and improper Automatic Gain Control (AGC) thresholds. Either of these would reduce the effective signal to noise ratios and dynamic range and thus the clutter suppression. However the data is still suitable for bias examination.

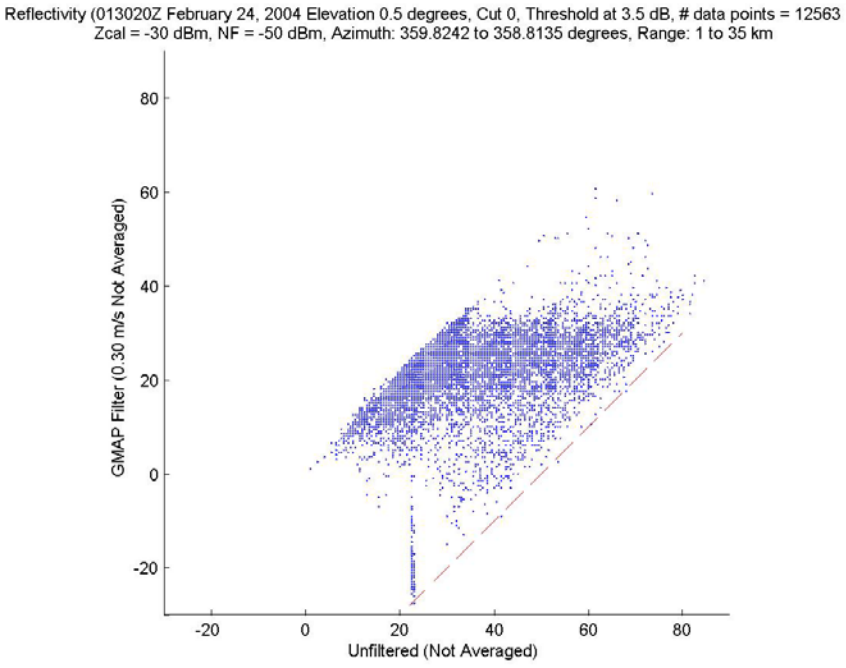

Figure 17 - Feb 24, 2004 Reflectivity Regression, Surveillance Scan

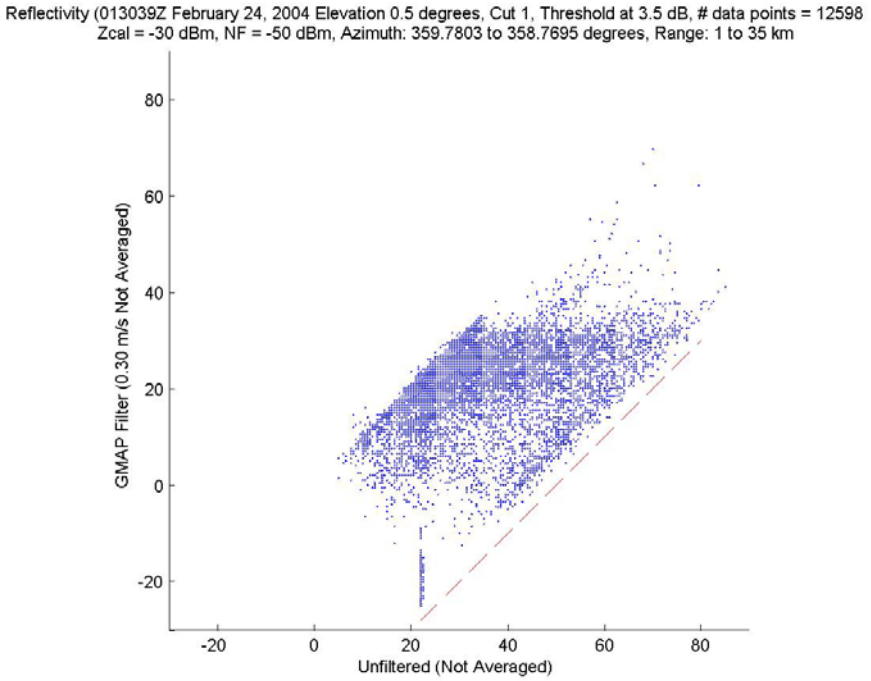

Figure 18 - Feb 24, 2004 Reflectivity Regression, Doppler Scan

GMAP induced velocity bias in the clutter region is shown in Figure 19. Maximum bias is about 1.8 ms^{-1} and is less than the requirement of 2.0 ms^{-1}.

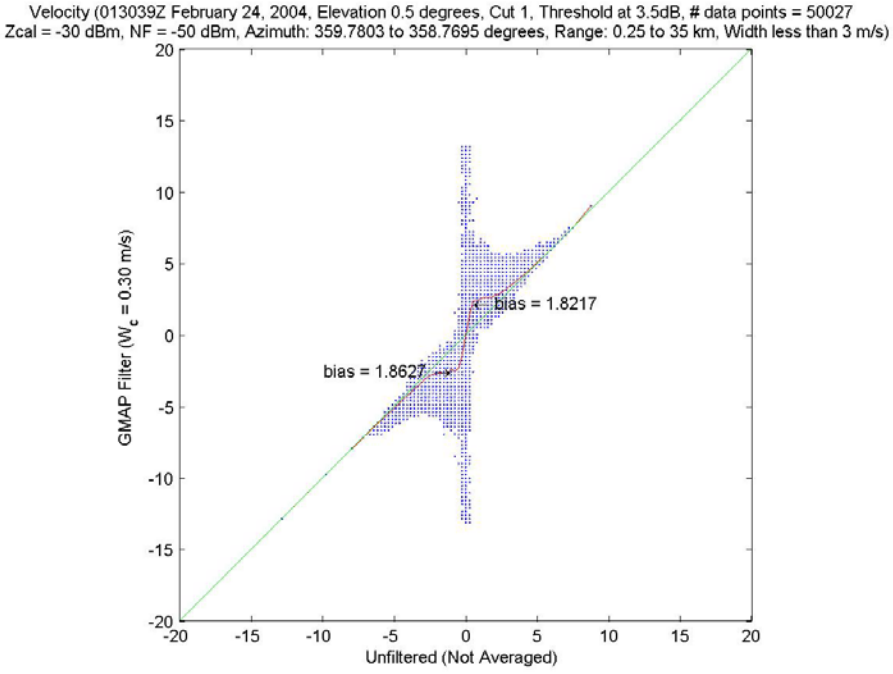

Figure 19 - Feb 24, 2004 Clutter Region Velocity Bias

A plot of unfiltered and filtered reflectivity against input velocity is shown in Figure 20 for the clutter region. Reflectivity and velocity are uncorrelated of course and this type of plot can be used to examine effects of GMAP on the reflectivity estimate. As can be seen there is a reflectivity estimate bias of about 5 dB extending about +/- 1 ms^{-1} from the zero isodop. This is larger than the 2 dB goal for the post correction scheme.

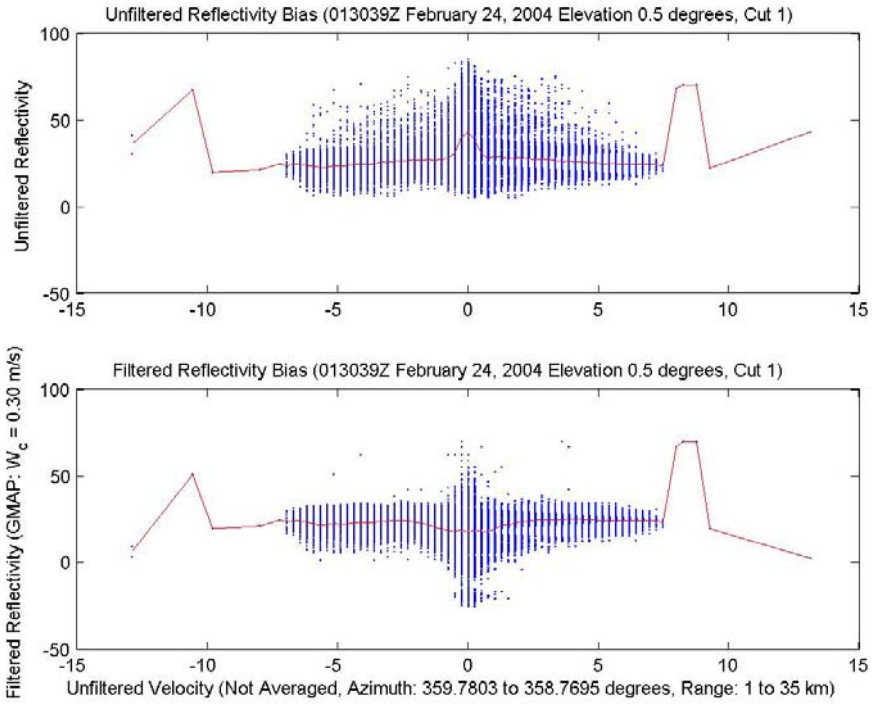

Figure 20 - Reflectivity/Velocity Regressions for Feb 24, 2004

For examination of GMAP effects operating on meteorological signal alone the region bounded by range greater than 40 km and less than 110 km with azimuth greater than 60 degrees and less than 280 degrees was selected. (This region is one of fairly uniform weather signal, but does encompass the zero isodop so that performance over a full range of velocities can be evaluated. The GMAP induced velocity bias for signal alone is shown in Figure 21. Maximum bias is less than 1 ms^{-1} (in the zero mean velocity region) and well within specifications.

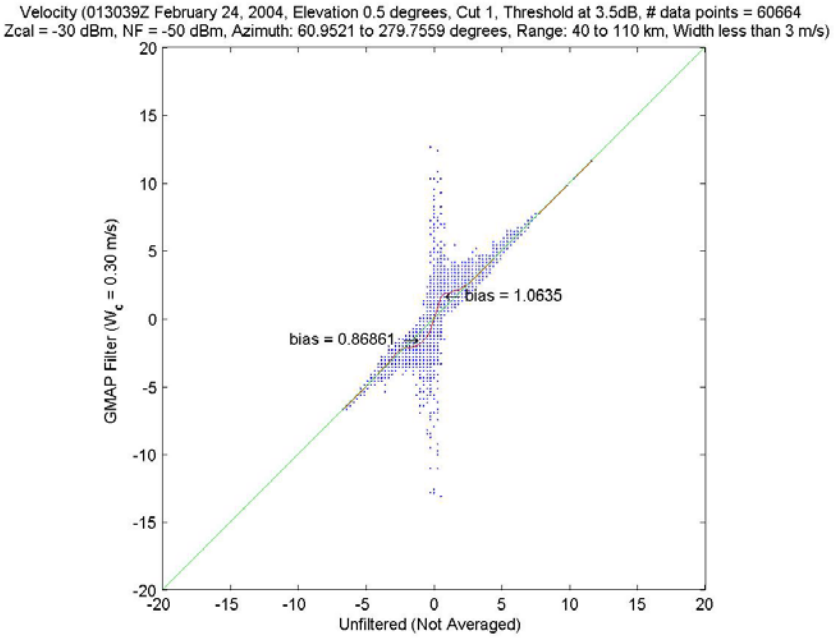

Figure 21 - Feb 24, 2004 Velocity Bias, Non Clutter Region

Differences in filtered and unfiltered reflectivity are shown in Figure 22. Maximum bias is about 7 dB and bias greater than 3 dB extends to about +/- 1.3 ms^{-1} from the zero isodop.

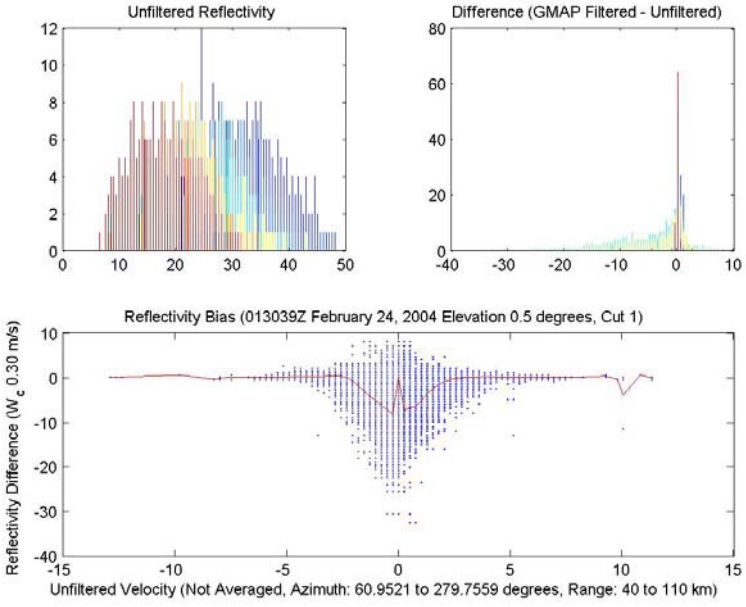

Figure 22 -Filtered vs. Unfiltered Reflectivity, Feb 24, 2004

- Case 3 – Clutter with Convective and Weak Signals (April 9, 2004)

A case of clutter and weak to moderate signal is shown in Figure 23, 24 and 25. There is convective meteorology from southwest to northwest at ranges greater than about 60 km and a small patch of anomalous propagation return to the southeast at range of about 75 km.

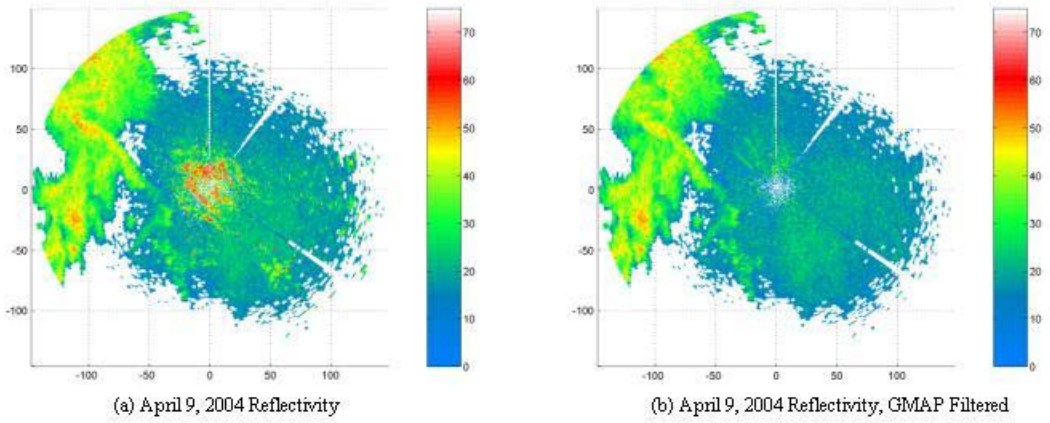

Figure 23 - April 9, 2004 Reflectivity Display

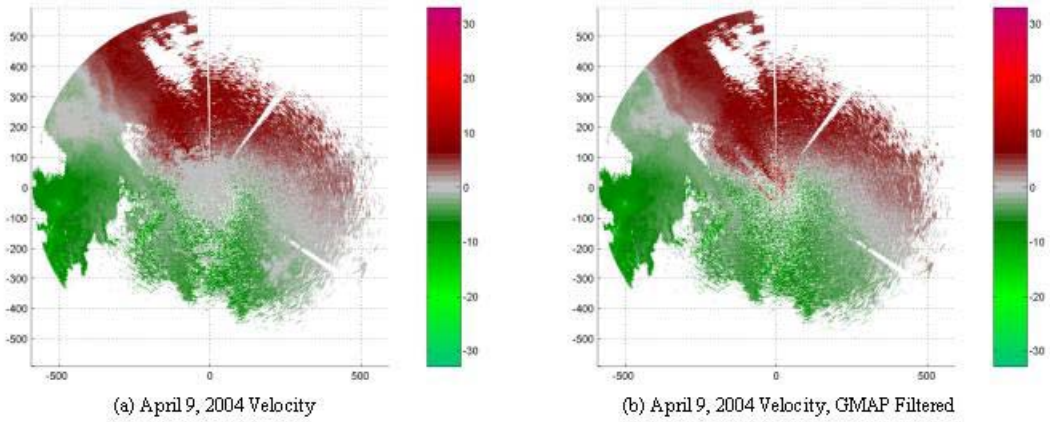

Figure 24 - April 9, 2004 Velocity Display

General characteristics of GMAP as seen from these displays are the same as previous and following cases. There is little clutter residue and substantial area recovered in both reflectivity and velocity fields. There is narrowing of the zero velocity isodop due to the upscale filter induced bias.

Suppression scatter grams for the surveillance and Doppler scans are shown in Figures 26 and 27. As seen, suppression exceeds 50 dB.

GMAP induced velocity bias for a combination of weak signal and clutter is shown in Figure 28. Maximum velocity bias is about 2.9 ms^{-1}, and occurs at about 0.5 ms-1. Note the sharp change in velocities across the zero isodop. This narrow region occurs from about –0.5 ms-1 to about 0.6 ms-1. In addition, the velocity bias does not exceed the required 2 ms-1 until the mean of the input velocity falls below 1 ms-1 showing that GMAP meets the System Specification (NTR) requirements in a high clutter region. Filtered reflectivity regressed on velocity for this same region is shown in Figure 29. Maximum reflectivity bias is about 2.0 dB, about the post-correction goal, and smaller than the February 24th case of 5 dB.

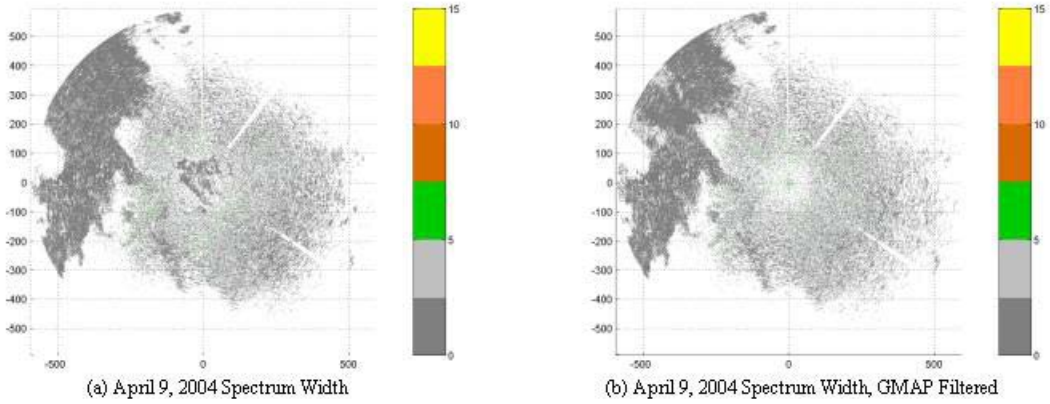

Figure 25 – April 9, 2004 Spectrum Width Display

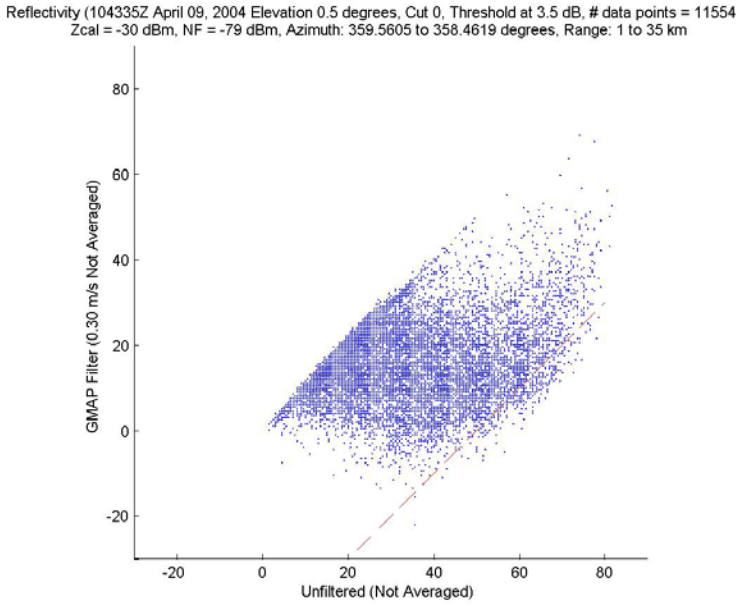

Figure 26 - April 9, 2004 Suppression, Surveillance Scan

GMAP performance in the convective meteorology region bounded by azimuth greater than 240 degrees but less than 330 degrees and range greater than 75 km but less than 148 km is shown in Figures 30 and 31. Maximum velocity bias is about 1.23 ms^{-1} and well within the 2 ms^{-1} required. Maximum reflectivity bias is about 5 dB and is greater than the post correction goal.

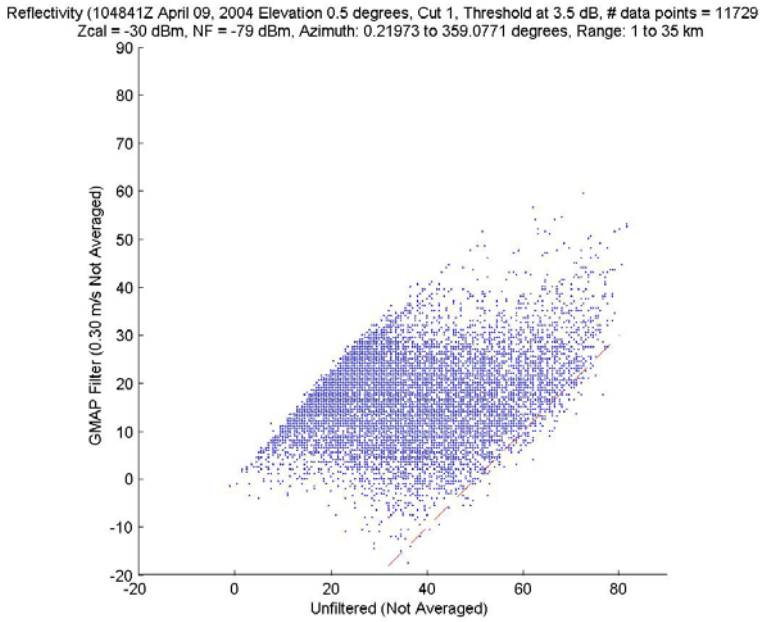

Figure 27 - April 9, 2004 Suppression, Doppler Scan

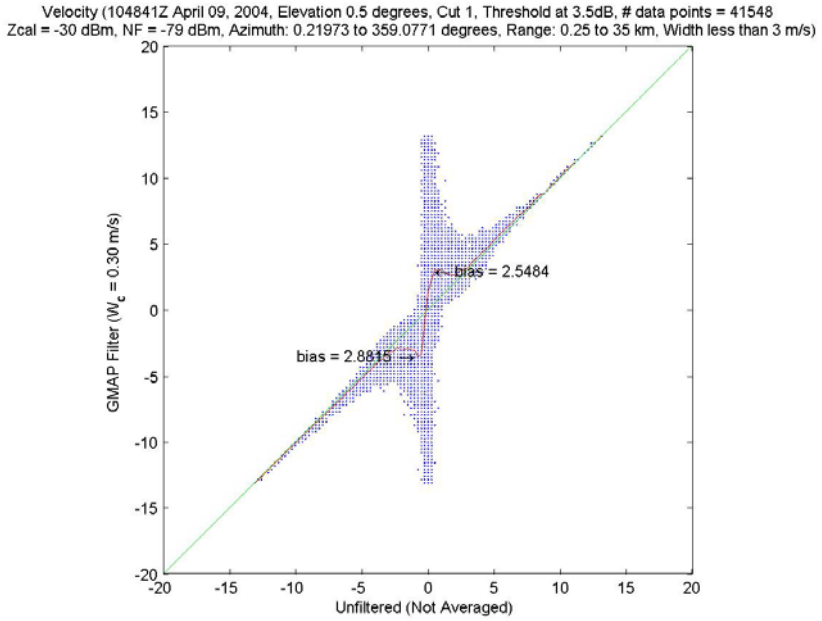

Figure 28 - April 9, 2004 Velocity Bias

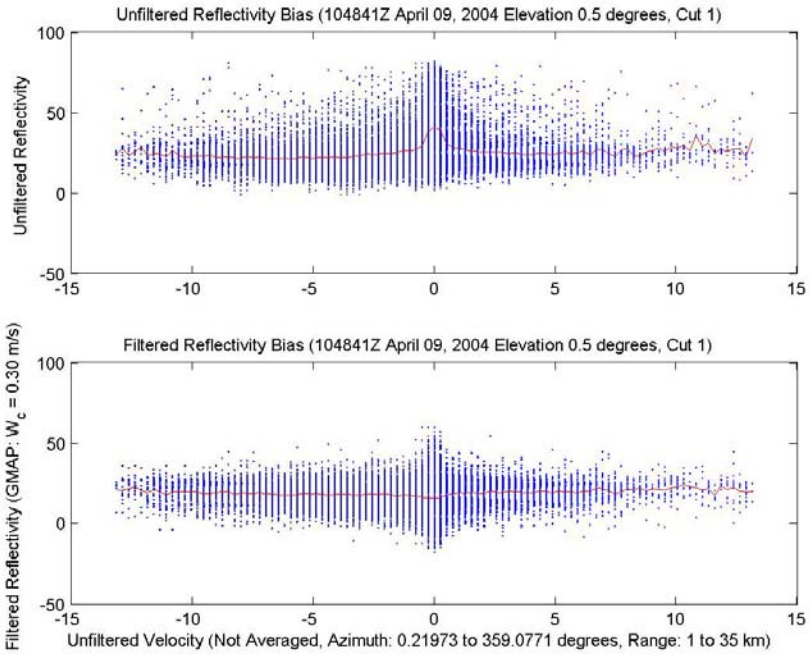

Figure 29 - April 9, 2004 Velocity - Reflectivity Regression

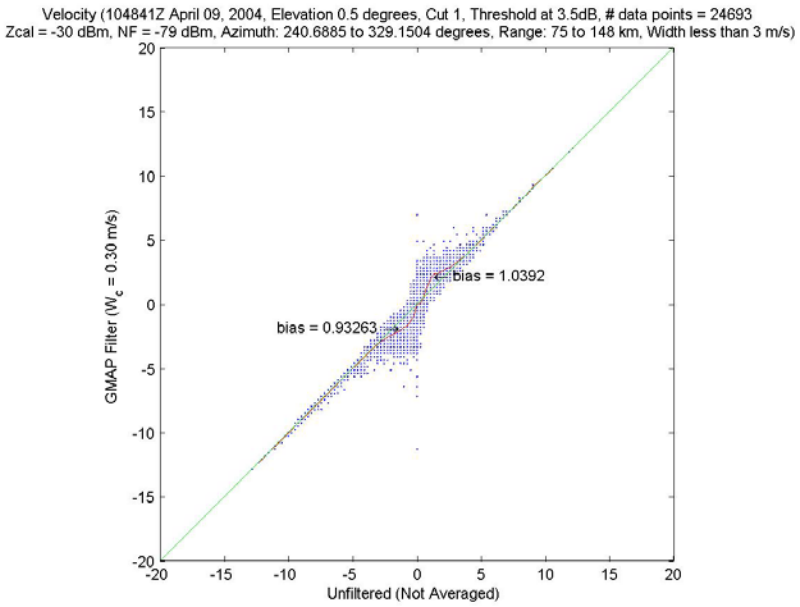

Figure 30 - April 9, 2004 Velocity Bias, Convective Region

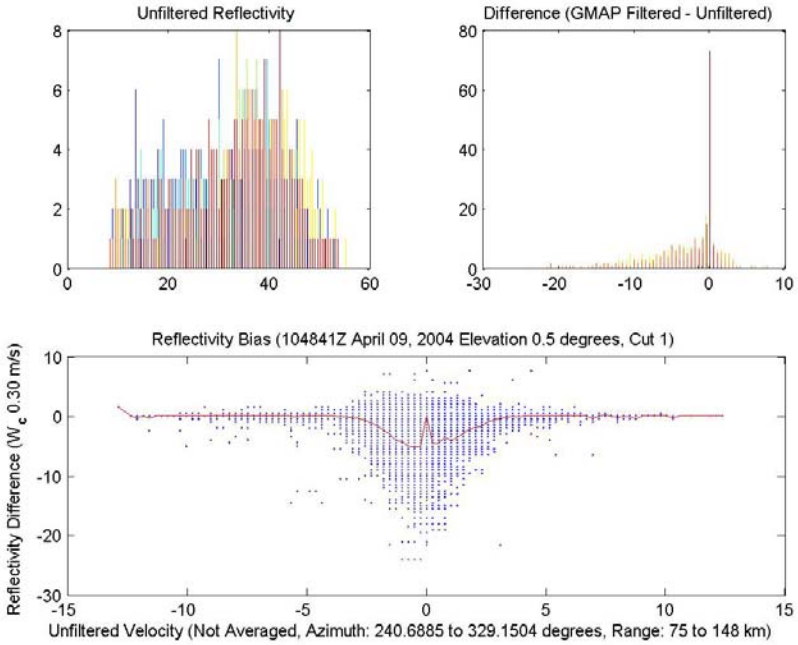

Figure 31 - April 9, 2004 Reflectivity Bias - Convective Region

7. Filter Sensitivity to Expected Clutter Filter Width Input

There is only one input parameter for the GMAP filtering which is the expected clutter spectrum width. The expected width is used in the initial modeling. However, the

algorithm is adaptive [2] and it is shown in the simulation study [1] that the initial value has little effect on filter performance, especially if the expected width is comparable to or larger than the actual width. If the expected width is smaller than the actual width, the filter is biased about 1.5 dB with strong clutter [1].

The expected width value effect, or lack thereof, on filter suppression is shown in Figure 32 for the case of April 17, 2004. By inspection, it is seen that there is essentially no difference in suppression for this range of expected widths as evidenced by the number of points to the right of the 50 dB lines. There is no discernable difference in suppression performance between expected widths of 0.1 ms^{-1}, 0.3 ms^{-1}, or 0.4 ms^{-1}.

(a) Expected Clutter Width = 0.1 ms^{-1}

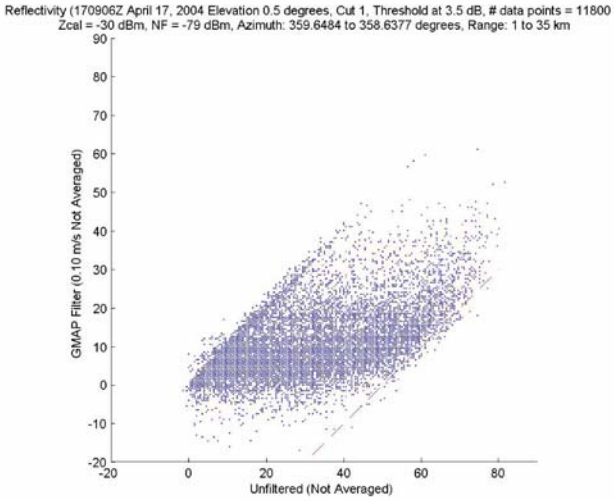

(b) Expected Clutter Width = 0.3 ms^{-1}

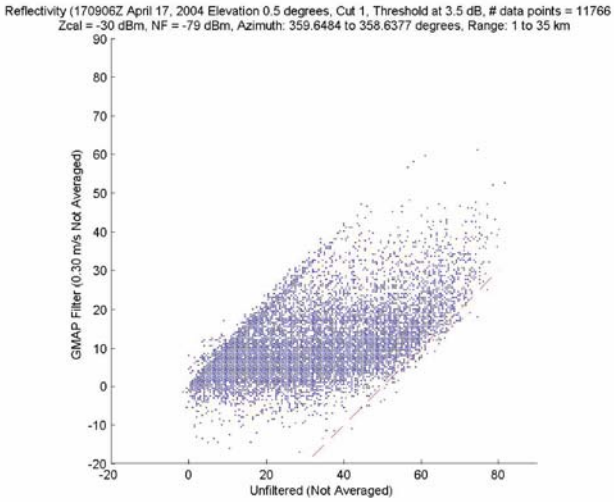

(c) Expected Clutter Width = 0.4 ms^{-1}

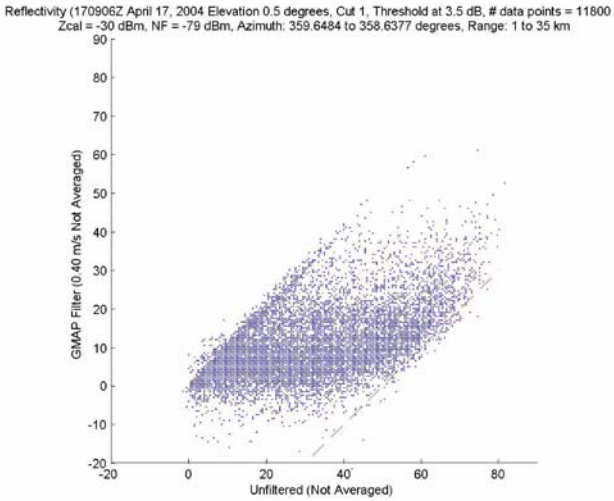

Figure 32 - Suppression Sensitivity to Expected Clutter Width, April 17, 2004

Filter induced velocity bias for expected widths of 0.1 ms^{-1}, 0.3 ms^{-1}, and 0.4 ms^{-1} is shown in Figure 33. Maximum bias is 2.8 ms^{-1} and only exceeds 2 ms-1 in the ragne of -1.0 ms^{-1} to 1.0 ms^{-1}. Peak bias and bias extent from the zero isodop is essentially the same for three expected widths. There are no discernable differences in velocity bias performance between expected widths of 0.1 ms^{-1}, 0.3 ms^{-1}, or 0.4 ms^{-1}.

Filter reflectivity bias (clutter residue in this case) is shown in Figure 34. As seen, there is no discernable difference in performance between the three expected widths.

The May 8, 2003 tornado case was also examined for seed value effects. A depiction of the difference between non filtered and filtered reflectivity for this case is shown in Figure 35. The color scale represents the level of suppression for each range cell. As seen, the level is zero for areas of weather free of clutter and maximum where the clutter was greatest (see Figure 7 for the unfiltered and filtered images). Several values of suppression above 50 dB can be seen.

Suppression, velocity bias, and reflectivity bias for this case are shown in Figures 36, 37, and 38 for expected widths of 0.1 ms^{-1} and 0.4 ms^{-1}. As seen, there is no discernable difference in performance for the two expected widths. Data for an expected width of 0.3 ms^{-1} is shown in the following section giving GMAP and legacy filter performance comparison using the May 8, 2003 case.

(a) Expected Clutter Width = 0.1 ms^{-1}

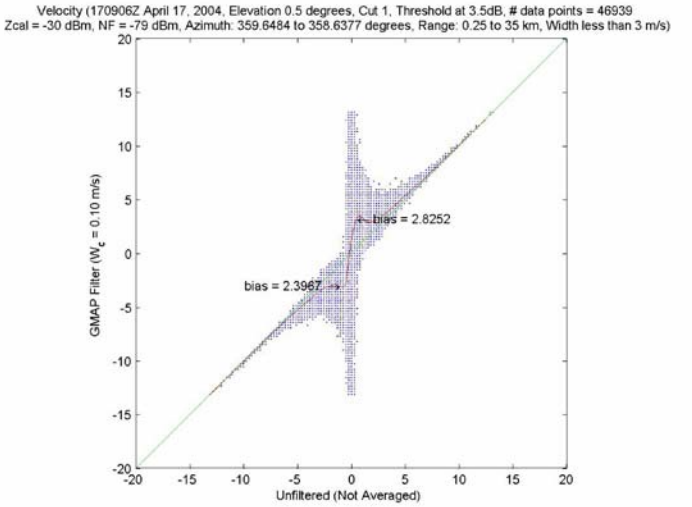

(b) Expected Clutter Width = 0.3 ms^{-1}

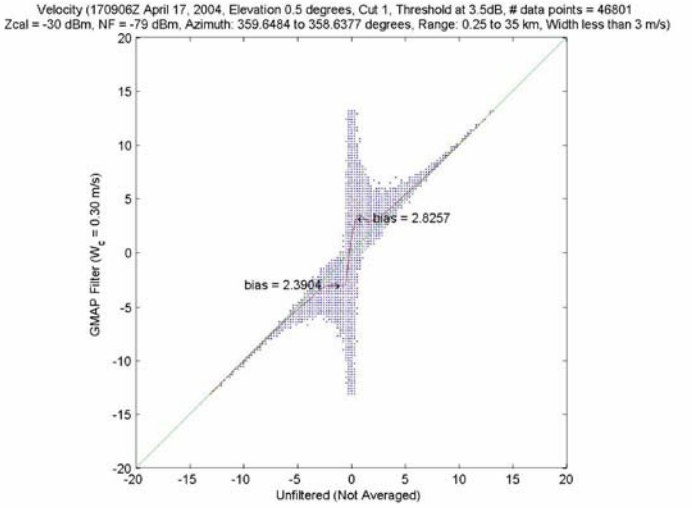

(c) Expected Clutter Width = 0.4 ms^{-1}

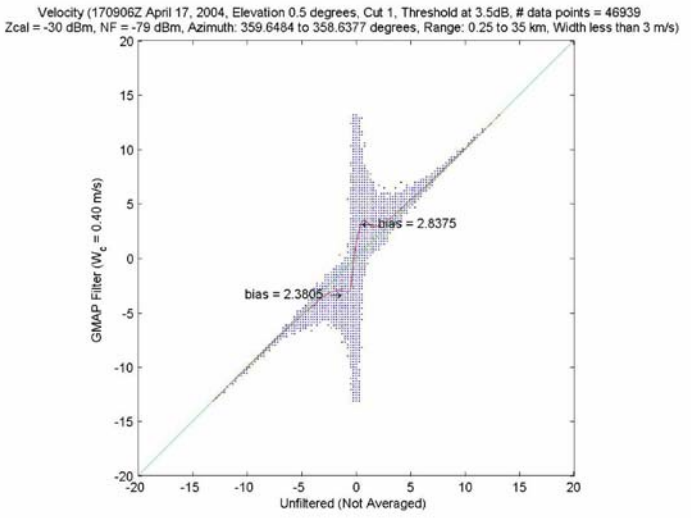

Figure 33 - Velocity Bias Sensitivity to Expected Clutter Width, April 17, 2004

(a) Expected Clutter Width = 0.1 ms^{-1}

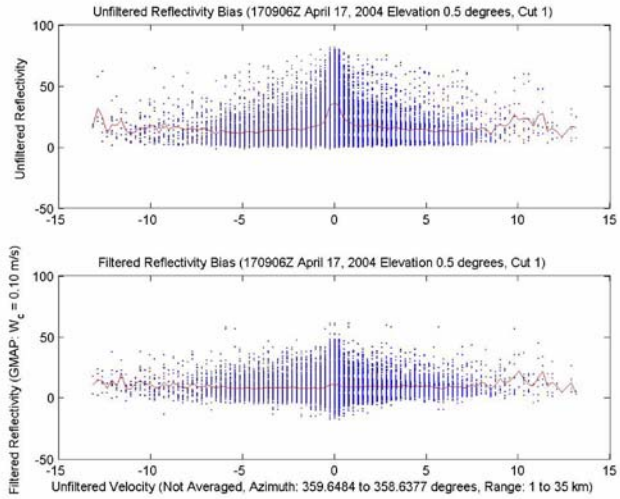

(b) Expected Clutter Width = 0.3 ms^{-1}

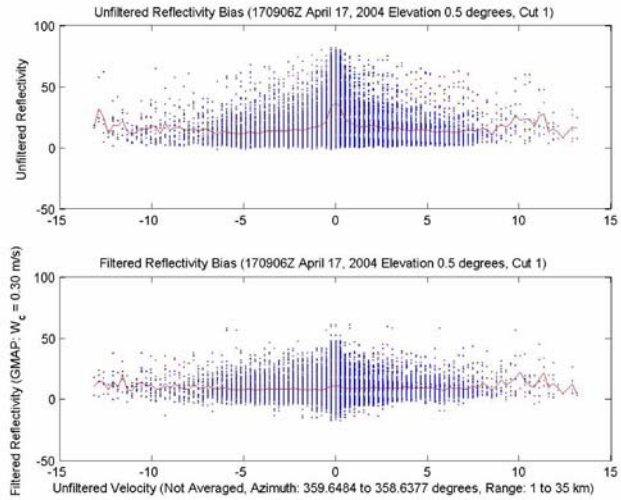

(c) Expected Clutter Width = 0.4 ms^{-1}

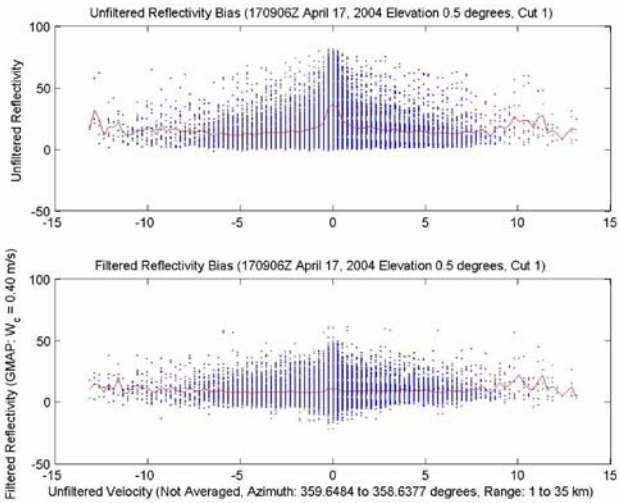

Figure 34 - Filter Induced Reflectivity Bias - April 17

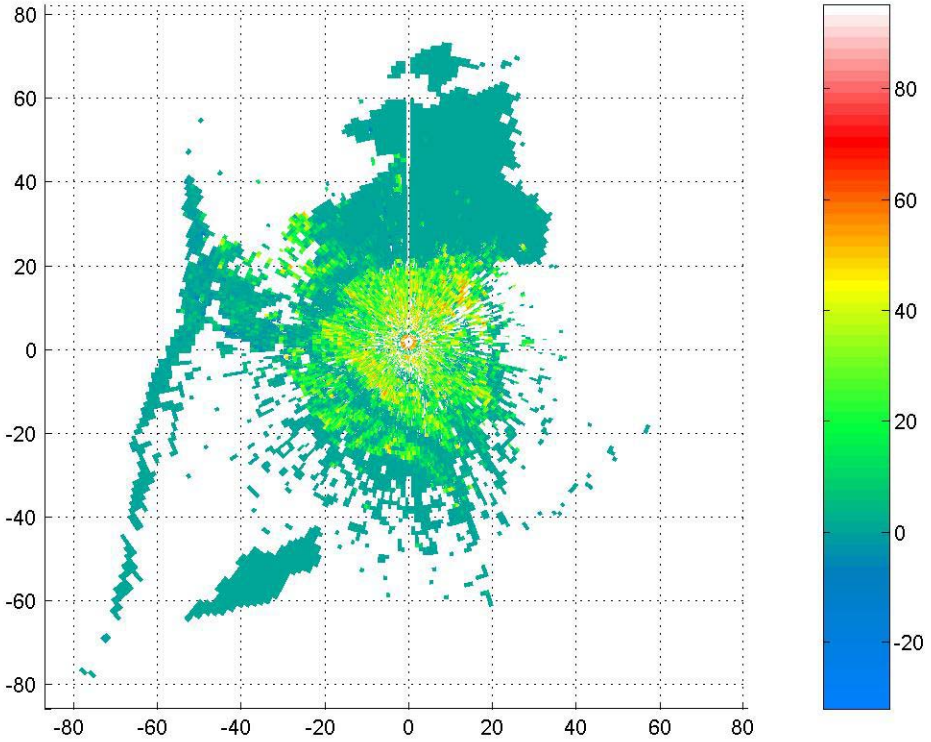

Figure 35 - Filter Suppression - May 8, 2003

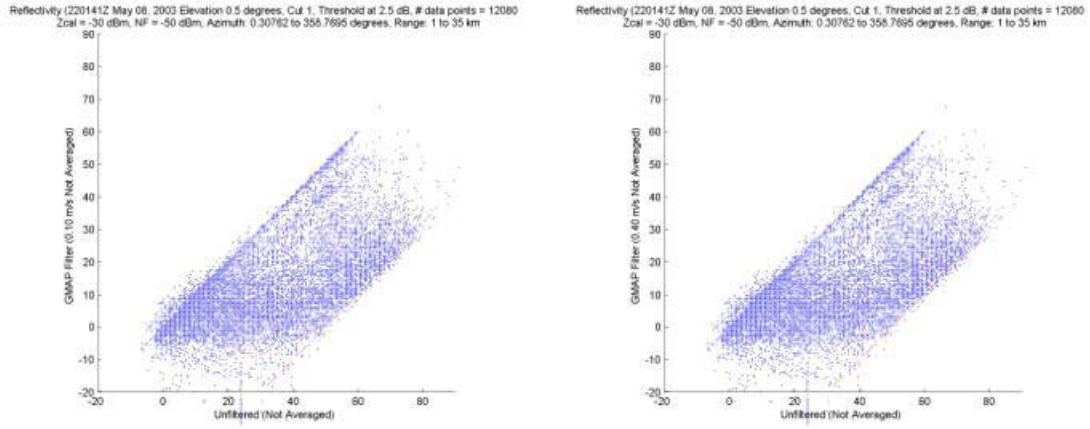

(a) Expected Clutter Width = 0.1 ms^{-1} **(b) Expected Clutter Width = 0.4 ms^{-1}**

Figure 36 - Suppression Sensitivity to Expected Clutter Width, May 8, 2003

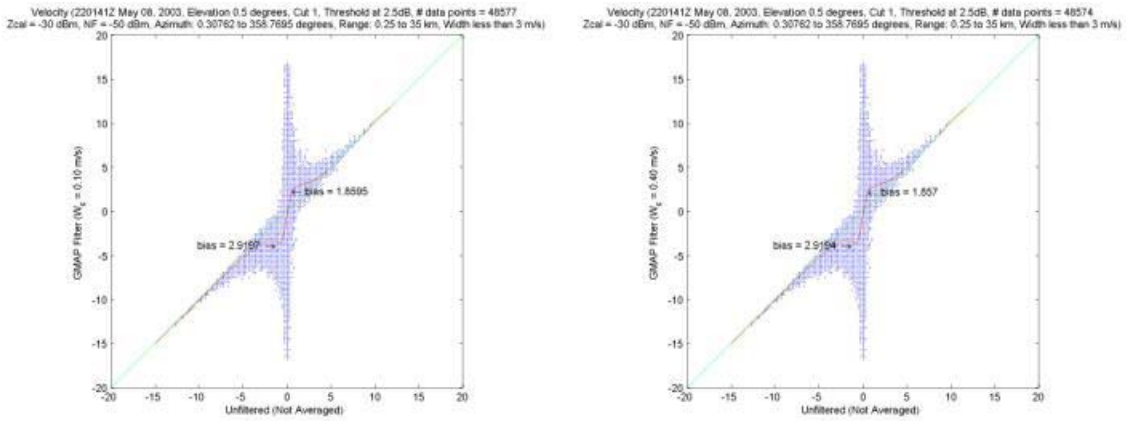

(a) Expected Clutter Width = 0.1 ms^{-1} **(b) Expected Clutter Width = 0.4 ms^{-1}**

Figure 37 - Velocity Bias Sensitivity to Expected Clutter Width, May 8, 2003

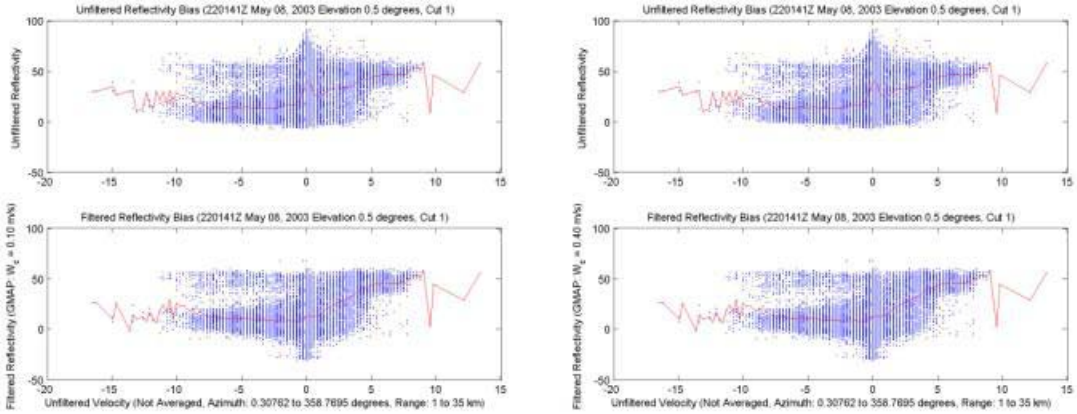

(a) Expected Clutter Width = 0.1 ms^{-1} **(b) Expected Clutter Width = 0.4 ms^{-1}**

Figure 38 - Reflectivity Bias Sensitivity to Expected Clutter Width, May 8, 2003

8. Increase in Standard Deviation of Spectral Moment Estimate

As noted in the simulation study [1], there is a GMAP induced increase in the standard deviation of the spectral moment estimate. This increase is most noticeable if operating on meteorology alone.

A special data set was collected on July 1, 2004 to support analysis of standard deviation. This data set consisted of a number of radials collected with the antenna stationary pointing at a fixed azimuths of either 142 (Doppler scan) or 291 (Surveillance

scan) degrees. Reflectivity and Velocity displays for this case and time of data collection are shown in Figure 39. This data for the Oklahoma City radar (KTLX) was obtained from NCDC. Reflectivity B-Scans for both the Surveillance and Doppler scans are shown in Figure 40. The plots show the average values for each range bin for all radials collected.

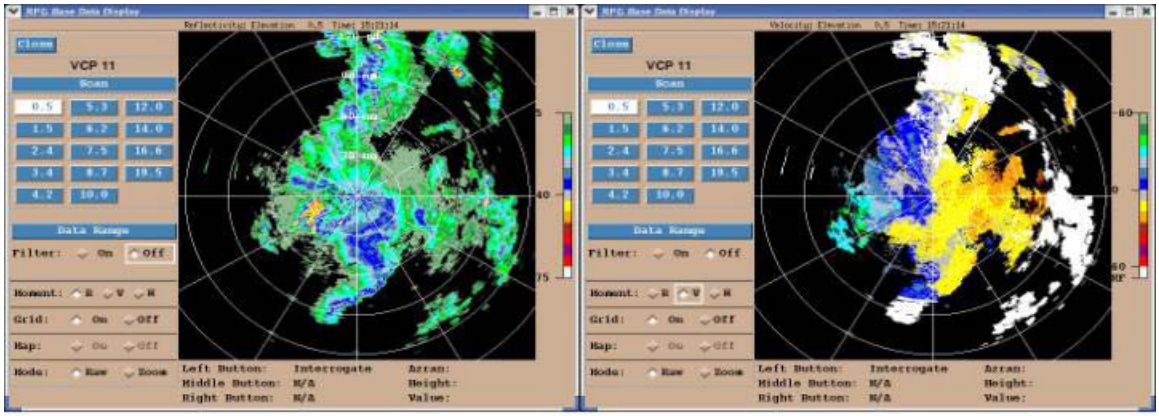

(a) July 1, 2004 Reflectivity

(b) July 1, 2004 Velocity

Figure 39 – Meteorology (KTLX Radar 152141Z), July 1, 2004

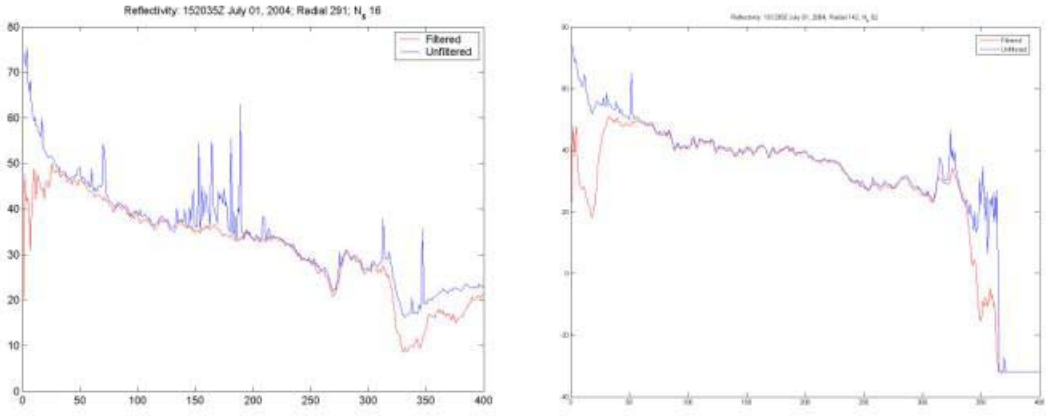

(a) Surveillance Scan, Radial 291, N = 16

(b) Doppler Scan, Radial 142, N = 52

Figure 40 - Reflectivity B-Scan, Average of Radials

The ratio of the reflectivity estimate standard deviation ratio with and without GMAP for the surveillance scan is shown in Figure 41 for 8 and 16 samples. Note that the ratio is 1.67 for both periodograms. Figure 42 gives the reflectivity standard deviation ratio for the Doppler scan using 20 to 52 samples. Note that the ratio is about

1.4 for all numbers of samples. Thus the estimate variance increase appears to have coherency (PRT, Width) dependency but not a dwell dependency.

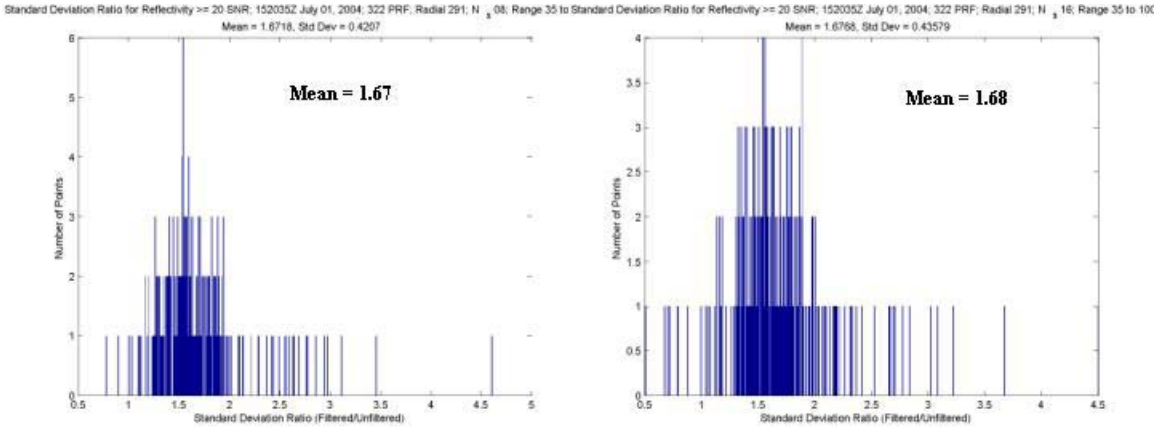

Figure 41 - SD Ratio, Reflectivity - Surveillance Scan July 1, 2004

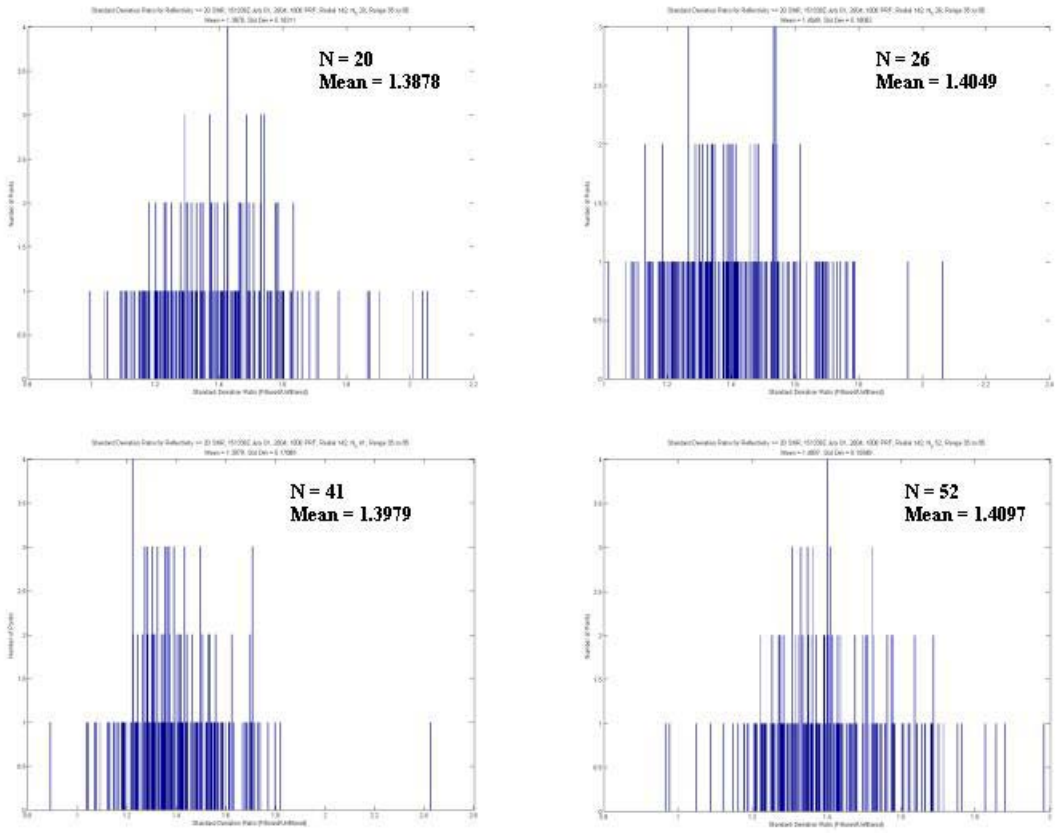

Figure 42 - SD Ratio, Reflectivity - Doppler Scan July 1, 2004

A Velocity B-Scan of filtered and unfiltered velocity estimates from the Doppler scan is shown in Figure 43 using 52 samples. The ratio of velocity standard deviation with and without GMAP filtering is shown in figure 44 for the Doppler scan and 20 to 52 Samples..

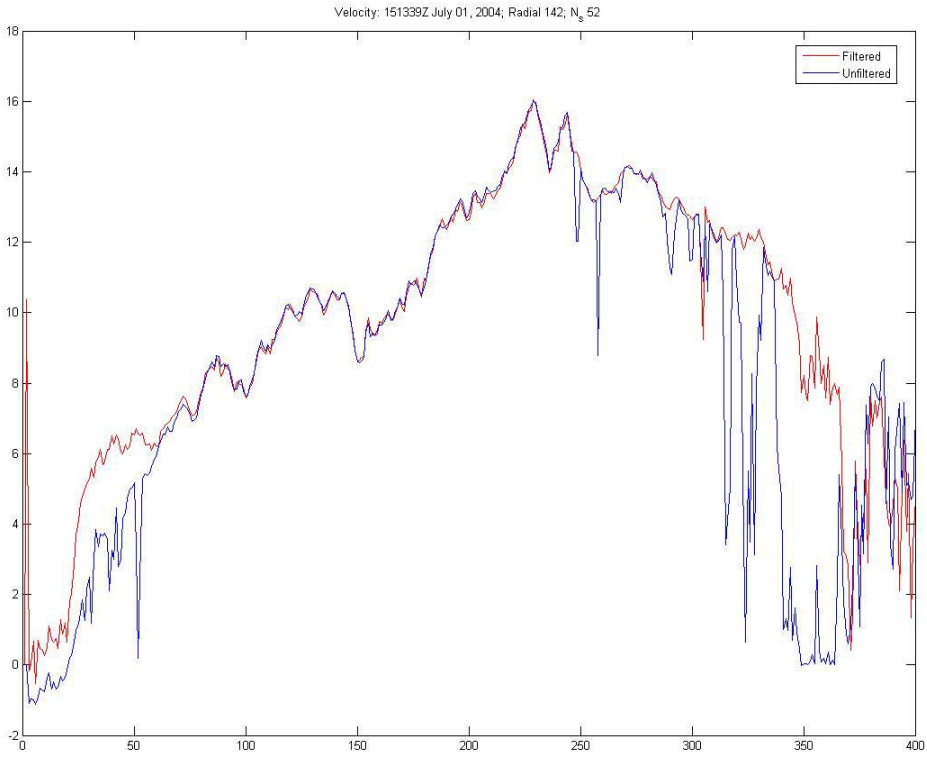

Figure 43 - Velocity B-Scan, July 1, 2004 KJIM Radial 142

Note that the SD ratio is about 1.4 (same as Doppler scan reflectivity) for all sample lengths in Figure 44. Again the fractional increase in velocity variance does not have a dwell time dependency. In the simulation study [1] (Section 9.0), a standard deviation ratio of 1.57 was noted for the given benchmark conditions. The difference between benchmark and this case is attributed to ratio coherency dependency. The filtered and unfiltered standard deviations are given in Figure 45. With 52 samples the velocity standard deviation is 0.7 ms^{-1} which implies a spectrum width of 2.25 ms^{-1} at the other benchmark condition [1]. Since correlation or coherency decreases with increasing

spectrum width it follows that the standard deviation ratio will increase with increasing spectrum width. From the assumed Gaussian correlation function

$$\beta(T_S) = \exp(-2\pi^2 w T_S^2)$$

where w is the Doppler frequency spectrum width (Hz) and TS is the sampling interval (sec) it can be estimated that the standard deviation ratio will increase to 1.67 for input spectrum width of 7 ms^{-1}, PRT of 1 ms, and Nyquist velocity of 26.6 ms^{-1}.

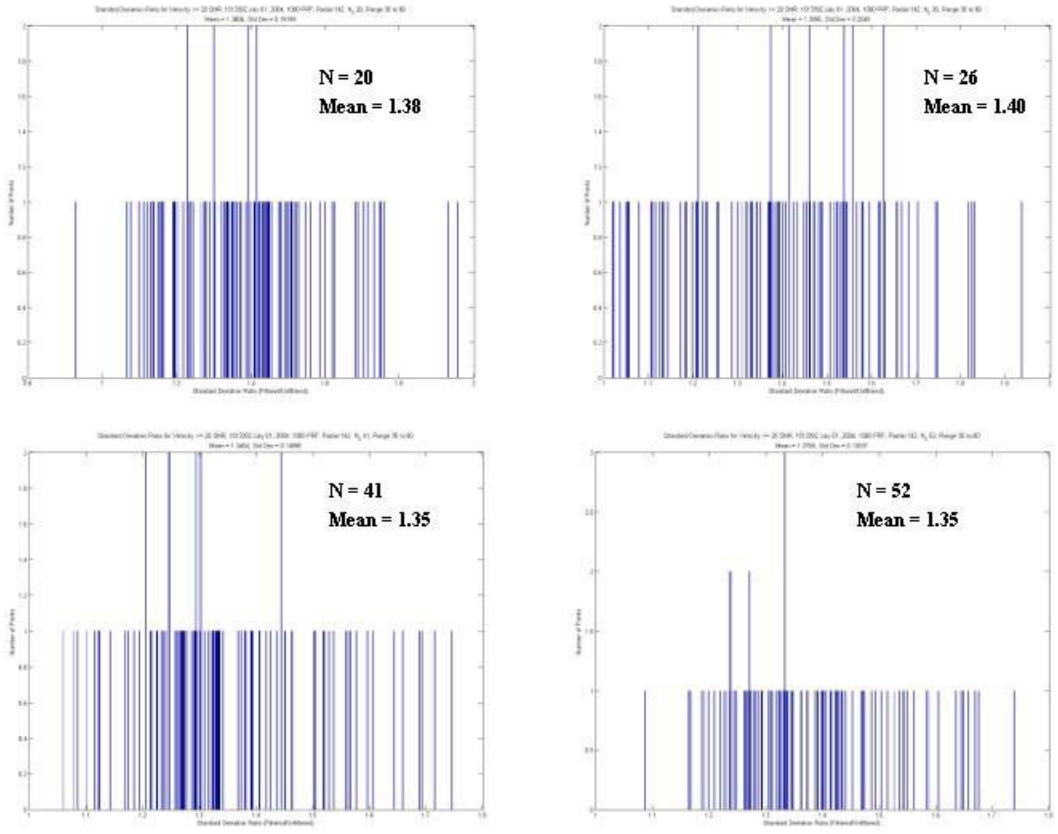

Figure 44 - Velocity SD Ratio, July 1, 2004, Doppler Scans

Signal simulation delivers a value of 1.70. Thus at PRT 5 the velocity standard deviation ratio will vary from about 1.35 for a spectrum width of 2 ms^{-1} to about 1.7 for a spectrum width of 7 ms^{-1}. The standard deviation ratio will be lower (less increase in standard deviation with filtering) at the higher PRF's due to the higher correlation.

More importantly, the variance increase supports the original recommendation [1] to invoke GMAP only when clutter is present i.e. only under clutter map control.

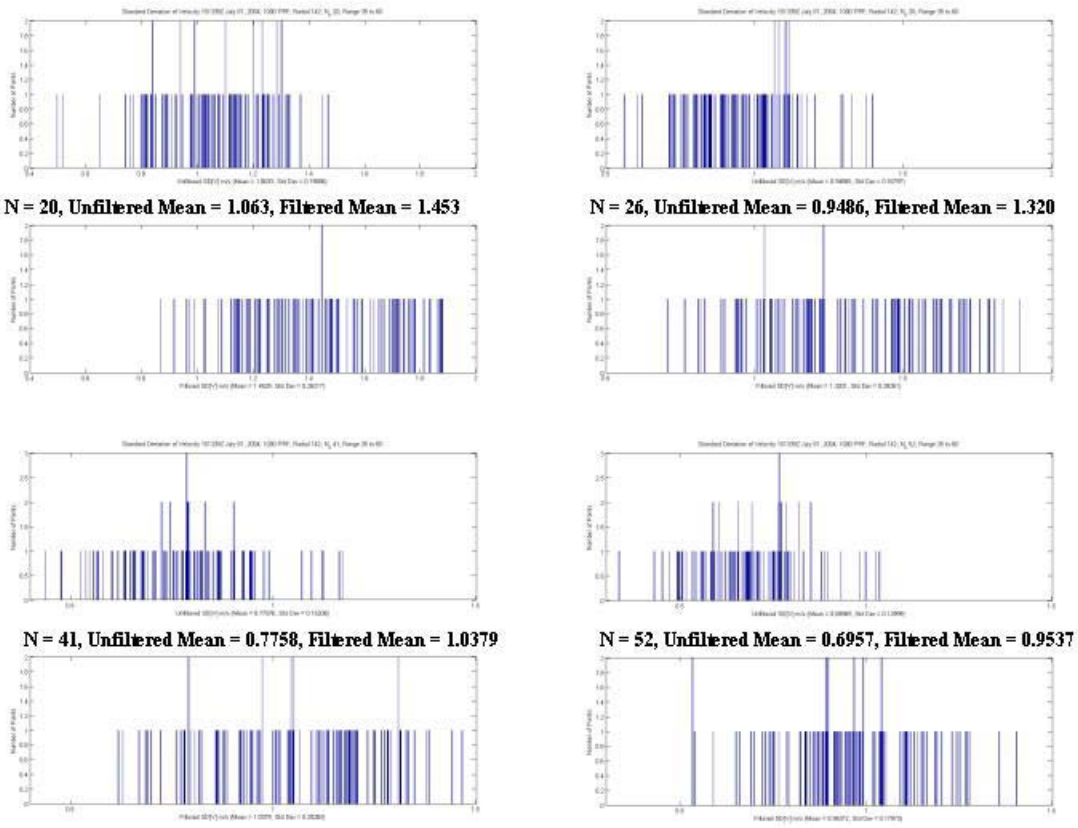

Figure 45 - Velocity Standard Deviations, Doppler Scan

9. Comparison of GMAP and the Legacy 5-pole Elliptic Filter

A data set taken May 8, 2003 is used in a comparison of GMAP and the legacy clutter filter. The reflectivity display for this case is shown in Figure 46. Note that in this particular case the GMAP suppression appears to be slightly greater than the legacy as evidenced by the clutter residue the southwest (Canadian River Ridge). Compared to GMAP there is also a slight reduction in area recovered by the legacy to the northwest but a slight increase to the southeast and southwest. Generally though, the visual performance is essentially the same for both filters.

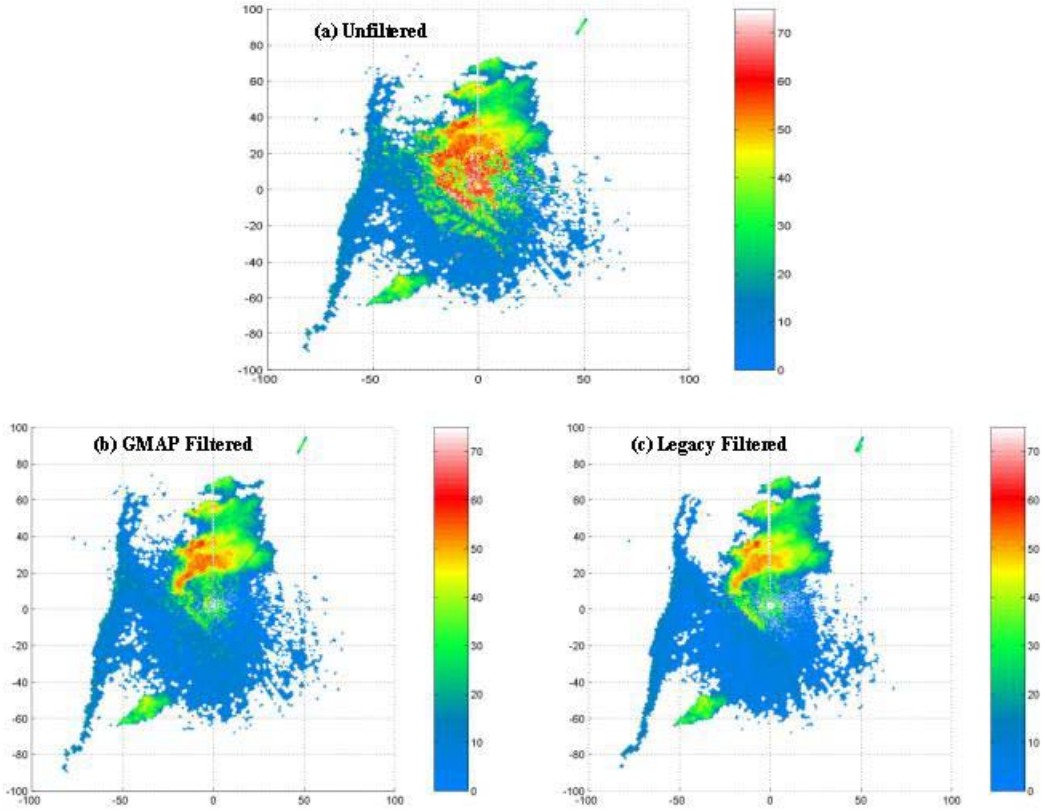

Figure 46 - Reflectivity May 8, 2003 - Legacy Comparison

The velocity display is shown in Figure 47. Again there is a slight increase in area recovered by the GMAP filter most notable to the east and west along the zero isodop. But overall the performance is essentially the same.

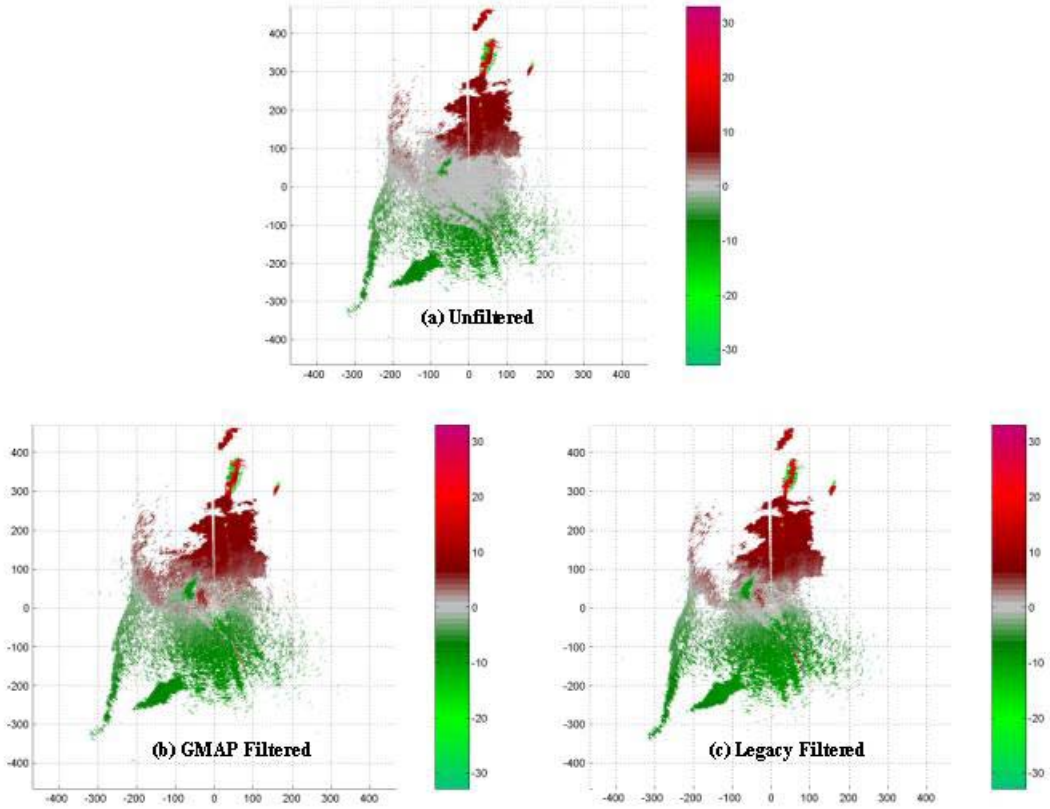

Figure 47 – Velocity May 8, 2003 - Comparison with Legacy Filter

Suppression scatter grams for the surveillance scan are given in Figure 48 Note that both filters deliver a suppression level of greater than 50 dB. However for the legacy filter there appears to be a slight decrease in the density of points slightly less than 50 dB. Again the performance is essentially the same for both filters.

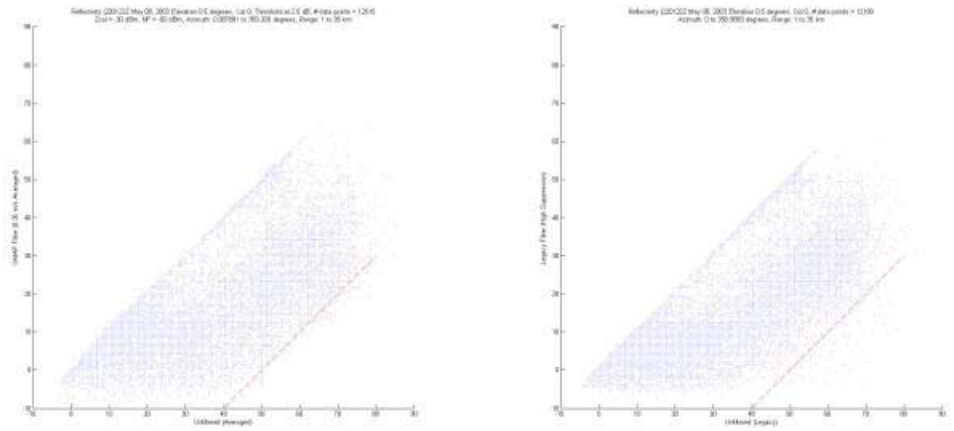

(a) GMAP Filtered (b) Legacy Filtered

Figure 48 - Reflectivity Scatter Grams - Filtered vs. Unfiltered

The reflectivity and velocity regressions for the surveillance scan are given in Figure 49. From the reflectivity trends over the velocity range of –2 ms^{-1} to + 2 ms^{-1}, the reflectivity bias due to clutter residue is estimated at about 5 dB for GMAP and about 8 dB for the legacy.

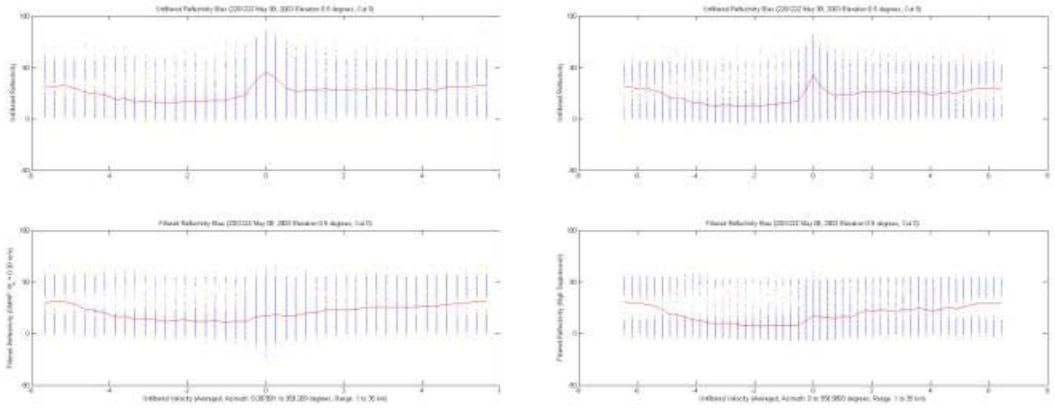

(a) GMAP Filtered (b) Legacy Filtered

Figure 49 - Regression, Reflectivity to Velocity - Filtered and Unfiltered

The regressions for the Doppler scan are shown in Figure 50. The bias is estimated at about 4 dB for both filters.

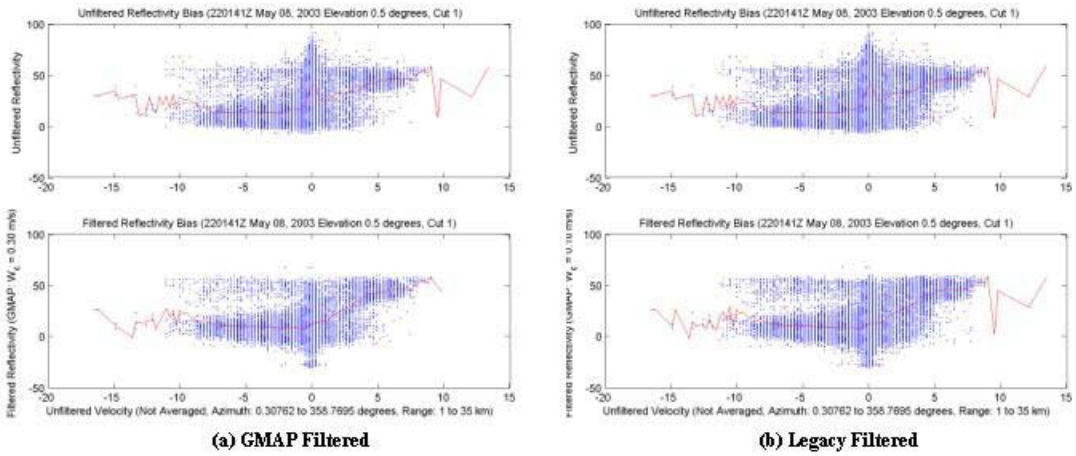

Figure 50 - Reflectivity vs. Velocity Regressions, Doppler Scan

The filtered – unfiltered velocity regression for the Doppler scan is given in Figure 51. Maximum velocity bias is estimated at 2.5 ms^{-1} for both filters.

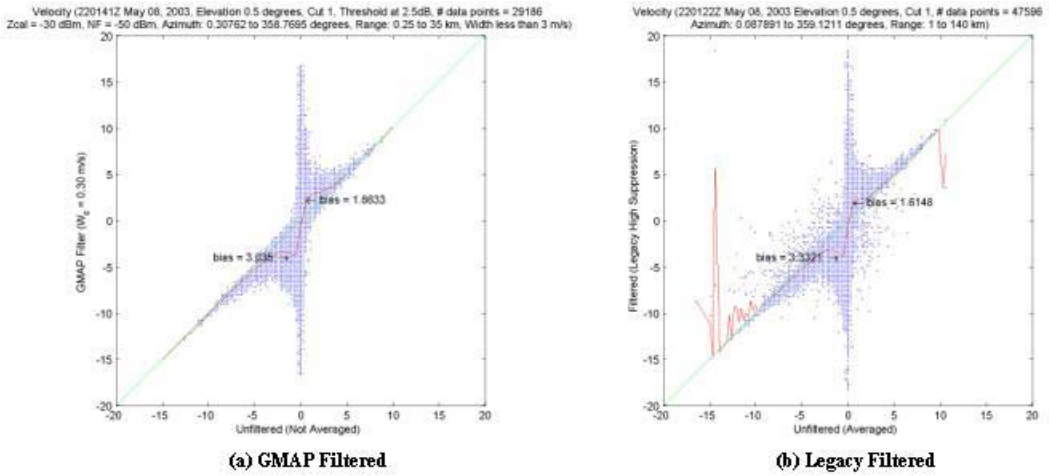

Figure 51 - Filtered vs. Unfiltered Velocity Regressions, Doppler Scan

The February 24, 2004 stratiform rain case was used for another example of GMAP and legacy filter comparisons. NSSL team members provided RRDA level 2 data for both the unfiltered and legacy 5-pole elliptic filtered reflectivity data. ROC engineers processed the same time series data set through the RVP8, producing equivalent unfiltered and GMAP filtered reflectivity images. Figure 52 presents the results.

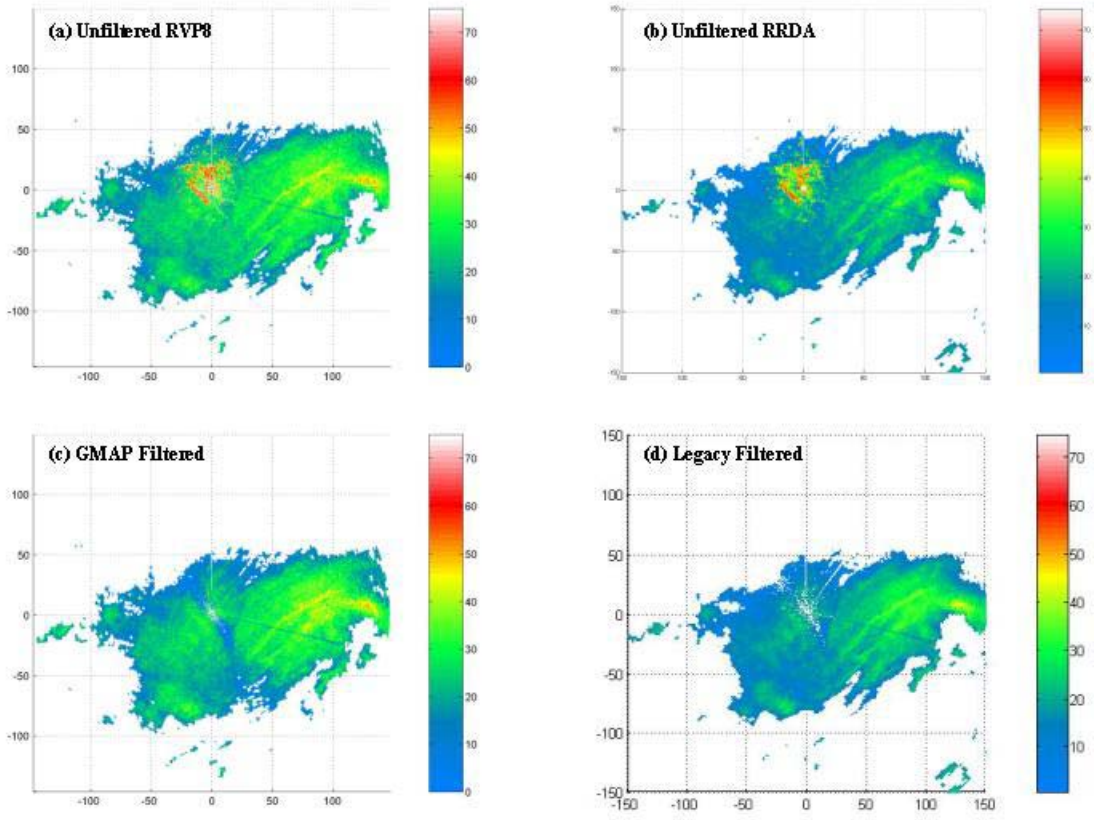

Figure 52 - Stratiform Rain Case Filter Comparison

Panels (a) and (c) in Figure 52 were produced by playback in the RVP8 and show the reflectivity data without filtering (a) and with GMAP filtering (c). A bias can be seen along the zero isodop line (see Figures 14 and 15 also). Panels (b) and (d) were produced from level 2 data supplied by NSSL. Their engineers used an off line program to process the same time series data in a manner replicating the legacy signal processor, producing RRDA level 2 moment outputs. From examination of the two sets of data, it is apparent that the RRDA processed data is much "cooler" than that produced by the ROC team on the RVP8. This is attributed to different settings for the reflectivity calibration constants and possibly by selection of different threshold values.

Accounting for the reflectivity calibration differences, the performance of the two filters is similar along the zero isodop, the region where the largest bias is expected. The legacy filter produces a slightly larger bias in this area, evidenced by areas of missing

values in the clutter region. This slightly higher bias is expected from the simulation study. Overall however, performance is similar.

10. Summary of GMAP Performance with Real Data

Operating on real data, the GMAP clutter filter algorithm exhibits the following performance.

GMAP meets and slightly exceeds the System Specification (NTR) requirement for clutter suppression levels of 50 dB. GMAP provides a routine suppression of 50 dB and a maximum suppression of about 55 dB (exhibited with data from the April 17, 2004, April 9 2004, and May 8, 2003 cases).

GMAP meets the System Specification (NTR) requirement for velocity bias contribution by the clutter suppression device of less than 2 ms^{-1}. In the absence of clutter (meteorological signal alone) the bias induced by the suppression scheme is about 1.05 ms^{-1} (Feb 24, 2004, April 9 2004 data sets). However, the velocity bias increases with clutter to signal ratio. For moderate clutter, the bias is about 1.8 ms^{-1} (Feb 24th) and for strong clutter the bias is about 2.8 ms^{-1} (April 9).

GMAP meets the System Specification (NTR) requirement for velocity standard deviation of less than 2 ms^{-1} by the clutter suppression device. GMAP increases the velocity standard deviation by a factor of 1.6 (July 1, 2004 data). Thus the benchmark standard deviation of 1 ms^{-1} is increased by only 0.4 ms^{-1}.

GMAP increases the standard deviation of the reflectivity estimate also. The increase is a factor of 1.67 in the surveillance mode and 1.4 to 1.7 depending on spectrum width in the Doppler mode.

GMAP meets the System Specification (NTR) for reflectivity bias if subject to the spectrum width, minimum usable velocity, and test criteria of the NTR.

GMAP does not meet the post correction reflectivity bias goal of less than 2 dB. (This is not a System Specification Requirement but a goal of the reflectivity bias post correction scheme for hydrology products.) In the clutter region, reflectivity bias ranges from about 2 dB (April 9, 2004) to about 5 dB (Feb 24, 2004, May 8, 2003). In the meteorological regions reflectivity bias ranges from about 5 dB (April 9, 2004) to about 7

dB (Feb 24, 2004). These bias values occur within a narrow region of mean velocities, typically between + and – 1 to 2 ms^{-1}, and are also typically less than that imposed by the legacy filters.

Performance is not very sensitive to the GMAP seed value for clutter spectrum width as expected from the simulation study. In fact, analysis with real data shows virtually no dependency on the seed width values.

11. Recommendations

- GMAP meets all operational requirements based on analysis with real data. Therefore, the study team recommends use of GMAP as the prime clutter suppression technique for the Open RDA.

- GMAP cannot maintain the ad hoc operationally acceptable reflectivity bias level goal (< 2 dB) for lower values of mean velocity and narrow spectrum widths. While the GMAP reflectivity bias performance is improved over that of the legacy notch filters, the study team recommends that post processing bias correction methods continue to be investigated.

- The team continues to recommend use of a clutter map and specific operator defined censor zones rather than the application of GMAP over the entire range of radar data.

- The team also recommends that the tools and techniques developed for this project continue to be applied to all new science enhancements considered for the ORDA.

12. Appendix A – References

[1] "Report on Open RDA – RVP8 Signal Processing, Part 1 – Simulation Study" R. Ice, D. Warde, D. Sirmans, D. Rachel, WS-88D Radar Operations Center Report, January 2004.

[2] "Gaussian model for adaptive processing (GMAP) for improved ground clutter cancellation and moment calculation" A. D. Siggia and R.E. Passarelli Jr., Preprint, Third European Conference on Radar in Meteorology and Hydrology, Visby, Island of Gotland, Sweden, 6 – 10 September, 2004.

[3] MATLAB is a general-purpose mathematics tool supplied by The Mathworks, Inc., and is fundamentally based on matrix operations. For detailed information and reference material on MATLAB see their web site at: http://www.mathworks.com/

[4] Technical Information on S-Pol can be found on NCAR's web site at: http://www.atd.ucar.edu/rsf/spol/spol.html

[5] "Plan for Evaluating New Science and Validating Open Radar Data Acquisition System (ORDA) Signal Processing", ROC Engineering Branch, Radar Engineering Team, August 13, 2003.

[6] "Test Plan for Evaluating Meteorological Suitability of ORDA SIGMET RVP8 Processor Output" ROC Applications Branch, March 22, 2004.

[7] "The Research Radar Data Analysis Tool (RRAT)" David L. Priegnitz, CIMMS/Univ. of Oklahoma, Norman, OK; and M. H. Jain. 20th International Conference on Interactive Information Processing Systems (IIPS) for Meteorology, Oceanography, and Hydrology.

13. Appendix B - Acknowledgements

Many individuals contributed to the successful completion of this study. The NSSL team led by Mike Jain provided excellent support in obtaining KOUN time series and RRDA level 2 data. Dan Suppes, Eddie Forren, and Dave Priegnitz were especially helpful in providing data and software utilities. The NSSL radar engineering team led by Allen Zahrai did some excellent work developing the level 1 recording capability and providing the signal processing routines for producing level 2 data. Overall, NSSL was quite supportive in providing opportunities for data collection with KOUN.

NCAR assisted with some time series data as well. They provided S-pol data sets and also located historical data from the 1997 Memphis collections. John Hubbert and Joe VanAndle were especially helpful.

Ron Guenther, support member of the ROC Software Engineering Team, provided the very useful tool for ingesting WSR-88D level 2 data into MATLAB and assisted with many valuable comments and suggestions.

Rick Rhoton and Darcy Saxion, support members of the ROC Radar Engineering team provided the RVP8 playback capability and also gave the study team valuable insight into the inner workings of the RVP8 signal processing software.

SIGMET Inc., representatives, provided excellent technical support, providing advice on RVP8 operational setup, answering technical questions, and investigating issues. SIGMET also generously provided temporary IRIS software licenses which greatly helped the ROC team remain on schedule. We are especially grateful for technical assistance from Richard Passarelli, Alan Siggia and Joe Holmes.

Lt. Ron Fehlen, former acting lead for the Radar Engineering Team, gave us unfailing management support and insightful technical leadership for this effort. We are in his debt.